Distinctive Oxidative Stress Responses to Hydrogen Peroxide in Sulfate Reducing Bacteria *Desulfovibrio vulgaris* Hildenborough

Aifen Zhou[1,2], Zhili He[1,2], Alyssa M. Redding[1,3], Aindrila Mukhopadhyay[1,3], Christopher L. Hemme[1,2], Marcin P. Joachimiak[1,4], Kelly S. Bender[1,5], Jay D. Keasling[1,3], David A. Stahl1[1,6], Matthew W Fields[1,7], Terry C. Hazen[1,4], Adam P. Arkin[1,4], Judy D. Wall [1,8], Jizhong Zhou[1,2 *]

Virtual Institute of Microbial Stress and Survival[1], Institute for Environmental Genomics, Department of Botany and Microbiology, University of Oklahoma, Norman, OK 73019[2], Physical Biosciences Division, Lawrence Berkeley National Laboratory, Berkeley, CA 94720[3], Earth Sciences Division, Lawrence Berkeley National Laboratory, Berkeley, CA 94720[4], Department of Microbiology, Southern Illinois University, Carbondale, IL 62901[5], Department of Civil and Environmental Engineering, University of Washington, Seattle, WA 98195-2700[6], Center for Biofilm Engineering, Department of Microbiology, Montana State University, Bozeman, MT 59717[7], and Biochemistry and Molecular Microbiology & Immunology Departments, University of Missouri, Columbia, MO 65211[8]

* Corresponding author: Dr. Jizhong Zhou

101 David L. Boren Blvd., SRTC

Institute for Environmental Genomics (IEG)

Department of Botany and Microbiology

University of Oklahoma

Norman, OK 73019

Phone: 405.325.6073, Fax: 405-325-7552

E-mail: jzhou@ou.edu

Running title: Oxidative stress response in *D. vulgaris*

ABSTRACT

Response of *Desulfovibrio vulgaris* Hildenborough to hydrogen peroxide (H_2O_2, 1 mM) was investigated with transcriptomic, proteomic and genetic approaches. Microarray data demonstrated that gene expression was extensively affected by H_2O_2 with the response peaking at 120 min after H_2O_2 treatment. Genes affected include those involved with energy production, sulfate reduction, ribosomal structure and translation, H_2O_2 scavenging, posttranslational modification and DNA repair as evidenced by gene co-expression networks generated via a random matrix-theory based approach. Data from this study support the hypothesis that both PerR and Fur play important roles in H_2O_2-induced oxidative stress response. First, both PerR and Fur regulon genes were significantly up-regulated. Second, predicted PerR regulon genes *ahpC* and *rbr2* were de-repressed in ΔPerR and ΔFur mutants and induction of neither gene was observed in both ΔPerR and ΔFur when challenged with peroxide, suggesting possible overlap of these regulons. Third, both ΔPerR and ΔFur appeared to be more tolerant of H_2O_2 as measured by optical density. Forth, proteomics data suggested de-repression of Fur during the oxidative stress response. In terms of the intracellular enzymatic H_2O_2 scavenging, gene expression data suggested that Rdl and Rbr2 may play major roles in the detoxification of H_2O_2. In addition, induction of thioredoxin reductase and thioredoxin appeared to be independent of PerR and Fur. Considering all data together, *D. vulgaris* employed a distinctive stress resistance mechanism to defend against increased cellular H_2O_2, and the temporal gene expression changes were consistent with the slowdown of cell growth at the onset of oxidative stress.

INTRODUCTION

Reactive oxygen species (ROS), including hydroxyl radical ($HO^{\cdot}$), superoxide radical ($O_2^{\cdot-}$) and hydrogen peroxide (H_2O_2), are natural products of aerobic metabolism and react easily with biological macromolecules including DNA, RNA, proteins and lipids (16). Single- and double-strand breaks in the DNA backbone, cross-links to other molecules, and lesions that block replication are examples of the deleterious effects of free radicals on DNA. Polyunsaturated fatty acids in the membranes can also be directly attacked by free radicals and the resulting decrease in membrane fluidity has a significant effect on membrane-bound proteins. Furthermore, the damaging effects of ROS can be amplified by the diffusion of secondary toxic messengers, such as aldehydes generated from the degradation of fatty acids. While the oxidation of proteins is relatively less well characterized, the deleterious consequences of modifications of proteins due to the attack of free radicals have been demonstrated in previous studies (8). Therefore, ROS is under very strict control in the cell through reactions with ROS-specific enzymes including superoxide dismutase (Sod), catalase (Kat), and nonspecific enzymes (e.g., alkyl hydroperoxide reductase, AhpCF). Furthermore, microbial cells also employ defense mechanisms such as DNA repair systems and proteolytic and lipolytic enzymes to limit and repair ROS damage (39).

Given the deleterious effect of ROS, much attention has been given to the molecular mechanisms and regulatory pathways involved in oxidative stress in *Escherichia coli* and *Bacillus subtilis*, two important model microorganisms. In *E. coli*, the transcriptional factors SoxR and OxyR respond to $O_2^{\cdot-}$ and H_2O_2 stress, respectively (31). The OxyR regulon includes genes involved in peroxide metabolism (e.g., *ahpCF*, *katG*, *dps*, etc.) and protection as well as genes involved in redox balance (*gor*, *grxA*, *trxC*) and important gene regulators such as *fur*. In response to peroxide challenge, *E. coli* OxyR undergoes a conformational change by forming an

intramolecular disulfide bond (24). The regulator OxyR is widely distributed in most Gram-negative bacteria as well as some Gram-positive bacteria. In organisms that lack OxyR, PerR was found to be a key transcriptional regulator (24). The PerR regulator was first identified in *B. subtilis* where it regulates the peroxide stress response. The PerR regulon of *B. subtilis* includes *kat, ahpCF, mrgA* (DNA protection), the *hemA* operon (heme biosynthesis), and *perR* itself (6, 7, 17, 34). In addition, *fur* (iron uptake and homeostasis) (3) and *zosA* (zinc uptake during peroxide stress) (19) are also under the regulation of PerR in *B. subtilis*.

While the facultative lifestyles of *E. coli* and *B. subtilis* justifies the presence of extensive oxidative stress response pathways, the presence of such complex pathways is more intriguing in the obligate anaerobic sulfate-reducing bacteria (SRB) *Desulfovibrio vulgaris* Hildenborough. In addition to the widespread ROS detoxification system (including Sod, KatA and the nonspecific peroxidase AhpC), *D. vulgaris* also has an alternative ROS defense system employing the Rbo/Rbr enzymes. Rbo (rubredoxin oxidoreductase) exhibits superoxide reductase activity and Rbr (rubrerythrin) exhibits NADH peroxidase activity (15, 26, 31, 41). Annotation of the *D. vulgaris* genome reveals ortholog of *B. subtilis perR* and two *perR* paralogs and *fur* and *zur,* but no orthologs of the *E. coli* OxyR and SoxR/SoxS regulators were identified. The reported aero-tolerance or aero-resistance of *D. vulgaris* is supported by the existence of genes constituting an oxygen reduction system including a membrane bound cytochrome *c* oxidase (*cox*, *DVU1811-1815*), a cytochrome *d* ubiquinol oxidase (*cydBA*, *DVU3270-3271*) and a cytoplasmic rubredoxin:oxygen oxidoreductase (*Roo*, *DVU3185*) (22). *Desulfovibrio* spp have been shown to tolerate low levels of oxygen and may even utilize oxygen as a terminal electron acceptor under certain conditions (27, 30), although growth of *Desulfovibrio* supported by oxygen respiration has not been reported.

Multiple studies have attempted to elucidate the mechanisms of the oxidative stress response in *D. vulgaris* (13-15, 36, 38, 46, 48) and use of different oxidative stress conditions has enabled the role of many of the oxidative stress genes to be discovered. For example, thiol-peroxidase, BCP-like protein and putative glutaredoxin were more abundant in *D. vulagris* cultures oxidated by continuous bubbling with pure oxygen, although enzymes involved in ROS detoxification such as Rbo(Sor), Rbr and Rbr2 were less abundant (13). Sor was shown to be a key player in oxygen defense under fully aerobic condition when *D. vulgaris* cells were stirred with a magnetic stirrer continuously in air (15). Roo enhanced survival of *D. vulgaris* under microaerophilic conditions (1% air) (46). In a study with low O_2 (0.1%) exposure (36), the role of PerR and its predicted regulon emerged where these genes comprised the few up-regulated genes in an otherwise unperturbed set of transcripts. However, no significant changes were reported in the expression of genes in the predicted PerR regulon in another study with *D. vulgaris* exposed to pure O_2 (38). Furthermore, genes *trx* and *trxB,* encoding thioredoxin and thioredoxin reductase that may constitute an alternative oxidative stress response mechanism, were found to be up-regulated or down-regulated in response to air or oxygen flushing, respectively (36, 38, 48). While these studies have improved our understanding of oxidative stress response in SRB, the genome-wide mechanistic picture of the *D. vulgaris* response remains elusive. A genome-wide analysis of *D. vulgaris* response to H_2O_2, known to be a more reactive oxidant than superoxide (33), was carried out to provide more insights into oxidative tolerance mechanisms in *D. vulgaris*.

In this study, a high-throughput transcriptomic analysis coupled with proteomic assays and mutagenesis approaches were used to monitor the transcriptional and translational changes of *D. vulgaris* in response to H_2O_2. Our results indicate that both PerR and Fur may play important

roles in the regulation of oxidative stress response genes in *D. vulgaris* and suggest that this bacterium may use the Rdl/Rbr2 and thioredoxin-dependent pathways in the detoxification of H_2O_2.

MATERIALS AND METHODS

Bacterial strains and growth conditions. *Desulfovibrio vulgaris* Hildenborough and deletion mutants of *fur* (JW707) and *perR* (JW708) were investigated in this study. Mutants were constructed as described in Bender *et al.* (4). Defined medium LS4D (35) with 50 mM lactate/60 mM sulfate was used as standard growth medium.

Hydrogen peroxide treatment. Bioscreen C (Growth Curves USA, Piscataway, NJ) was used to test the effect of H_2O_2 on the growth of *D. vulgaris* cells. A series of different concentrations of H_2O_2 (0.5, 1, 2, 4, 8 and 10 mM, prepared from 30% [vol/vol] H_2O_2 [Sigma, 9.8M] with anoxic H_2O) were added to mid-log phase cell cultures grown in a 100-well plate in Bioscreen C and the growth was monitored as the absorbance at 600 nm. To produce biomass for the transcriptomics and proteomics assays, *D. vulgaris* cells were pre-cultured in the LS4D with a 1% (vol/vol) inoculum and grown to mid-log phase (6 X 200-ml cultures in 250-ml bottles). The cells were then subcultured into production vessels (2000 ml in 2-liter glass bottles placed in the anaerobic chamber in the 30 ^{o}C incubator) in triplicate with 10% (vol/vol) inocula. H_2O_2 was added to mid-log phase cultures (an OD_{600} of 0.35) to a final concentration of 1mM. Biomass (300 ml) was harvested at 0 min (just before treatment), and at 30, 60, 120, 240, and 480 min after H_2O_2 treatment. All sampling occurred in the anaerobic chamber. Samples were pumped through stainless steel tubing in ice-water into centrifuge bottles surrounded by ice and stored on ice in the anaerobic chamber before centrifugation.

Oxidative stress response of deletion mutants of *D. vulgaris fur* and *perR* were also investigated in this study. Biomass was produced as mentioned above and harvested at two time points - 0 min and 120 min after 1 mM of H_2O_2 treatment.

RNA isolation, cDNA synthesis and fluorescence labeling. Total cellular RNA was isolated using TRIzol reagent (Invitrogen, Carlsbad, CA) and purified using the RNeasy Mini kit (QIAGEN, Valencia, CA). On-column DNaseI digestion was performed with the RNase-free DNase set (QIAGEN, Valencia, CA) to remove possible genomic DNA contamination. Ten μg of purified total RNA was used to generate Cy5-dUTP (Amersham Biosciences, Piscataway, NJ) labeled cDNA target (44). Cy5-labeled cDNA was purified with QIAGEN QIAquick PCR purification kit. The quality and quantity of the Cy5-labeled cDNA target were measured by Nanodrop at wavelength 260 nm (for DNA concentration) and 650 nm (for Cy5). The Cy5-labeled cDNA target was dried and stored at -20^{o}C.

Genomic DNA isolation and fluorescence labeling. Genomic DNA (gDNA) was extracted from *D. vulgaris* cultures as described previously(50). The extracted DNA was labeled with the fluorophore Cy3-dUTP (Amersham Biosciences, Piscataway, NJ) and the Cy3-labeled gDNA was purified with QIAquick PCR purification kit. The amount of gDNA for each labeling reaction was 1.5 μg and the resulting Cy3-labeled gDNA from one labeling reaction was used for 3 hybridizations. The quality and quantity of the Cy3-labeled gDNA target were measured by Nanodrop at 260 nm (for DNA concentration) and 550 nm (for Cy3), and the target was dried and stored at -20 ^{o}C.

Microarray hybridization and data analysis. The *D. vulgaris* whole-genome oligonucleotide microarray constructed with synthesized 70mer oligonucleotide probes covers 3,482 of the 3,531 protein-coding sequences of the *D. vulgaris* genome (21). The quality of this

microarray in global transcriptional profiling has been extensively validated in previous studies (9, 10, 21). Array hybridizations and data analysis are performed as described previously (21, 35). Briefly, the pooled Cy3-labeled gDNA was used as control and co-hybridized with each Cy5-labeled sample and hybridizations were carried out in a TECAN HS4800 (TECAN Group Ltd, Durham, NC). After 10 hrs of hybridization at 45°C with 50% formamide in hybridization buffer, the microarray slides were dried and scanned for the fluorescent intensity using the ScanArray Express microarray analysis system (Perkin Elmer, Boston, MA). The fluorescence signal intensities for each spot were calculated with the software ImaGene version 6.0 (Biodiscovery, Marina Del Rey, CA) using 16-bit TIFF images. The data processing was done as described by Mukhopadhyay et al. (35). The heat-maps of gene expression data were graphed using Cluster 3.0 and Treeview (12). Absolute correlation (uncentered) was used as the similarity metric and complete hierarchical clustering was performed. Microarray data for this study are available at http://www.microbesonline.org/cgi-bin/microarray/viewExp.cgi?expId=123 (GSE14345) and http://www.microbesonline.org/cgi-bin/microarray/viewExp.cgi?expId=1258 (GSE4355).

DCA (detrended correspondence analysis) was used to analyze the similarity of transcription profiling between different time points. Compared to the gene expression at time zero, the ORFs with more than two-fold changes in gene expression (|Log2R|>1.0, |Z|>1.5) for at least one of the time points were kept for analysis. Five sets of data for control samples, C30-C480, and 5 data sets for treatment samples, T30-T480, were included in the analysis. The $\log_2$R value was transformed to fold change. It was set to one for genes with no expression changes detected. There were a total of 1488 ORFS considered. DCA was run with software PC-ORD (version 4, MjM Sortware Design).

Construction of gene co-expression network. The microarray data from all six timepoints were used for the construction of the gene co-expression network based on the random matrix theory approach (32). First, all raw fluorescent intensities were normalized by the Cy3 signals generated from genomic DNA controls (35). Second, for each spot, a ratio (Cy5/Cy3) of the Cy5 signal to the Cy3 signal was calculated and then logarithmic transformation of the ratio was performed. Third, a gene expression ratio of a treatment to a control was calculated by randomly dividing a treatment Cy5/Cy3 ratio by a control Cy5/Cy3 ratio. All the datasets at each time-point were used for the gene co-expression network identification. The gene co-expression network presented here was generated with the cutoff of Pearson correlation coefficient of 0.95 between each pair of genes, which was determined by the network identification method (32).The sub-module was separated by fast greedy modularity optimization (11, 37).

Proteomic analyses. Biomass harvested at 120 min after the addition of 1 mM H_2O_2 was used for proteomic analysis to reveal the response at the protein level. Sample preparation, chromatography, and mass spectrometry for iTRAQ proteomics were performed as described previously (40) with modifications to the lysis buffer used. Briefly, frozen cell pellets from triplicate 50 ml cultures were thawed and pooled prior to cell lysis. Cells were lysed via sonication in 4 M urea with 500 mM triethylammonium bicarbonate, pH 8.5 (Sigma-Aldrich), and the lysate, separated by centrifugation at 4^{o}C 15,000 *g* for 30 min, was used as total cellular protein. Eighty micrograms of proteins were taken from each sample, denatured, reduced, blocked, digested, and labeled with isobaric reagents as per manufacturer's directions (Applied Biosystems). The 1 mM H_2O_2-treated samples were labeled with tag_{114} or tag_{117} which provided a technical replicate to allow assessment of internal errors; the control was labeled with tag_{115}. Then, the iTRAQ-labeled samples were separated into 21 salt fractions via strong cation

exchange (SCX). The fractions were desalted, dried, and separated on a C_{18} reverse phase nano-LC-MS column with a Dionex LC system coupled with an ESI-QTOF mass analyzer (QSTAR® Hybrid Quadrupole TOF, Applied Biosystems, Framingham, MA) as previously described (40).

Collected mass spectrograms were analyzed using Analyst 1.1 with Protein Pilot 1.0 (Applied Biosystems). Protein identifications were confirmed using MASCOT version 2.1 with the FASTA file containing all the ORF protein sequences of *D. vulgaris* (1) as the theoretical search database. The same parameters were used in both programs; namely, trypsin was the cleavage enzyme, and mass tolerances of 0.1 for MS and 0.15 for MS/MS were used. Peptides with charges from +2 to +4 were searched. All matches above a 95% confidence interval were considered. Scripts were written using Python to collate data between Run 1 and Run 2 and between MASCOT and Protein Pilot. Only proteins identified by at least two unique peptides were considered for further analysis. All protein ratios were obtained from Protein Pilot. Tag ratios for each protein are a weighted average from peptides of all confidence that are uniquely assigned to that protein. To compute the level of significant changes, z-scores were computed for all $\log_2$ values. Protein $\log_2$ values with z-scores $\geq |2|$ were considered to be significantly changed. Each sample was run in duplicate to control for internal error. Reported protein ratios are an average of the internal and external technical replicates (4 samples in total) with standard deviations.

RESULTS

The growth of *D. vulgaris* cells was affected by the addition of H_2O_2. In order to identify an effective concentration of H_2O_2 treatment for the investigation of the oxidative stress response at

both transcription and translation levels, different concentrations of H_2O_2 (0, 0.5, 1, 2, 4, 8, and 10 mM) were tested for their effects on cell growth. Low concentrations of H_2O_2 (0.5 ~ 2 mM) showed about 3 hrs delay of growth (1 mM, Fig. 1A), while 4 mM or higher concentrations of H_2O_2 arrested growth for a proportionately longer times (data not shown). Therefore, 1 mM of H_2O_2 was chosen for further experiments in this study. To gain insights into the temporal pattern of the stress response at the gene transcription level, biomass was harvested at 5 time-points (30, 60, 120, 240 and 480 min) after H_2O_2 treatment for transcript analysis.

The temporal pattern of transcript changes in response to H_2O_2. Extensive gene expression changes after H_2O_2 treatment were detected by the *D. vulgaris* whole genome microarray. In terms of gene number and fold change, the transcriptional response reached a peak (Fig. 1B) at 120 min after H_2O_2 treatment with 485 genes up-regulated and 527 genes down-regulated, representing approximately 14% or 15% of the total open reading frames on the array, respectively. DCA analysis showed that the gene expression profiles of control (C30 – C480) and treatment (T30 – T480) samples were clearly separated by axis 1. The early (T30, T60 and T120) and late responses (T240 and T480) to H_2O_2 treatment were well separated as well (Fig. 1C).

In terms of gene categories, at 30 min after the addition of H_2O_2, genes involved in "posttranslational modification, protein turnover, chaperones" and "general function prediction" had greatest differential expression (Fig. S1); at 60 min, besides the two gene categories mentioned above, many more genes were significantly changed, including genes involved in COG functional groups for: signal transduction mechanisms; energy production and conversion; cell envelope biogenesis; outer membrane; amino acid transport and metabolism; cell motility and secretion; and DNA replication, recombination and repair (Fig. S1). The most dramatic

changes of gene expression level were observed at 120 min (Fig. S1). “Signal transduction mechanism” and “posttranslational modification, protein turnover, chaperons” were the two categories with the highest number of up-regulated genes. “Energy production and conversion” and “amino acid transport and metabolism” were gene categories with highest number of down-regulated genes. In contrast, fewer genes with expression changes were detected at both 240 and 480 min, which was consistent with the restoration of normal growth.

When the gene expression level changes were considered, *nspC* (involved in amino acid transport and metabolism), *DVU3136* (a nitroreductase gene), *DVU2442* (encoding a heat shock hsp20 family protein) were examples of the most up-regulated genes (Table S1); and the corresponding genes in the same operon *speA-lys1-nspC(DVU0417-0419)*, *DVU3135(mdaB)-DVU3136*, *DVU2441(hspC)-DVU2442* were all up-regulated after H_2O_2 treatment; *flgG* (cell motility) and *DVU0359* (encoding a HesB-like domain protein) were two examples of most up-regulated single gene operons. *frdC* (*DVU3261*, fumarate reductase, cytochrome b subunit) was an example of the most down-regulated genes, and two other genes, *frdA* and *frdB* in the same operon were also down-regulated (Table S1).

Gene co-expression network in response to H_2O_2. In order to further understand the oxidative stress responses at the whole genome scale and to gain insights on the functions of hypothetical proteins, all microarray data were used to construct a gene co-expression network by a novel random matrix theory-based approach (38). The resulting network contains a total of 175 genes that were partitioned into 5 sub-networks (modules, with more than four genes) with the Pearson correlation coefficient cutoff of 0.95 for each pair of genes (Fig. 2). Module 1 is the largest module including 155 genes involved in different gene categories; Modules 2-5 are small

modules with 4-8 genes. As expected, genes from the same operon tend to link together in the sub-networks and all modules contain functionally coherent sets of genes (Fig.2).

Microarray data suggests that a genome-wide response was triggered by the addition of oxidant H_2O_2. It is conceivable that genes involved in DNA repair, protein turnover, lipid metabolism, energy metabolism and other cellular activities are all coordinately regulated, which was shown as a complex oxidative stress response network in Module 1 (Fig. 2) (Table S2). Module 1 can be further divided into sub-modules (1-1 to 1-6) using the modular identification program (11, 37). The major gene categories in sub-module 1-1 were "energy production and conversion" and "translation, ribosomal structure and biogenesis". Genes predicted to be involved in energy production and conversion such as *atpG* (*DVU0776*), *atpA* (*DVU0777*), *atpF1* (*DVU0780*) and *dsrMKJOP* (*DVU1286-1290*) were tightly linked with genes involved in "translation, ribosomal structure and biogenesis" such as *DVU1308-1311* via connections of genes (*fabF* (*DVU1204*), *accC* (*DVU2226*)) involved in lipid metabolism. All of these genes had decreased gene expression. Negative correlations were found between *DVU3136* (nitroreductase, increased gene expression) in sub-module 1-2 and down-regulated genes in sub-module 1-1. The major gene category in sub-module 1-3 was "posttranslational modification, protein turnover, chaperons". Genes belong to this gene category such as *trxB* (*DVU1457*), *msrA* (*DVU1984*), *msrB* (*DVU0576*), *dnaJ* (*DVU1876*), *DVU2441-2442* (heat shock proteins) were linked together.

The gene co-expression network provides an advantage for functional prediction of hypothetical genes due to the fact that functionally related genes are connected to each other in the gene co-expression networks (32). Therefore, unknown function genes *DVU1875*, *DVU1601*, *DVU2282* in sub-module 1-3 could be functionally involved in "posttranslational modification, protein turnover, chaperons". For the same reason, *DVU1601* and *DVU2310* (general function

prediction only) in sub-module 1-3 may have a possible function in protein modification and turnover (Fig. 2).The Clps domain in DVU1601 also supports its possible function in protein modification or turnover.

The major gene category in Module 2 was posttranslational modification, protein turnover, and chaperons, and the network topology suggested that two hypothetical genes *DVU0241* and *DVU0242* could be related to such functions. Interestingly, iron transportation protein gene *feoB* (*DVU2571*) was correlated to these genes whose expression was significantly up-regulated (Fig. 2; Table S2). Genes in Modules 3 to 5 were related to energy production and conversion. In Module 3, the expression of all these genes was down-regulated except *rdl* (*DVU3093*, rubredoxin-like protein, predicted oxidative stress response gene) that was up-regulated (Table S2). Again, hypothetical gene *DVU3032* in Module 3, and *DVU0035* and *DVU0263* predicted to encode a tetraheme cytochrome c3 protein in module 4 could be involved in energy production and conversion.

The gene co-expression network not only provided us high-level view of the stress response in *D. vulgaris*, but also shed light on the importance of genes in the response network based on the number of links for each gene. When challenged with H_2O_2, the gene expression for H_2O_2 scavenging enzyme, NifU and MsrAB related damage repair, thioredoxin-dependent pathway increased, while that for sulfate reduction, protein synthesis and ATP production decreased. Many genes involved in various categories had more than 6 connections (Table S2). For example, genes are actively involved in sulfate reduction (*DVU1286*, 9; *DVU1288*, 9), ATP production (*DVU0776*, 11; *DVU0777*, 11), protein synthesis (*DVU1309*, 9; *DVU1310*, 9; *DVU1311*, 8), thioredoxin-dependent pathway (*DVU1457 (trxB)*, 8), *DVU1144* (transcriptional regulator, 10), and damage repair (*DVU1984 (msrA)*, 7) and several genes encoding ribosomal

proteins. Especially, as one of the top 20 most up-regulated genes with 6 connections, *DVU3136* may play an important role in the stress response of *D. vulgaris* as its homologue in *E. coli* (5, 29).

The proteomic response to H_2O_2. To understand the *D. vulgaris* response to oxidative stress at the protein level, the iTRAQ proteomics strategy was used to assess changes in proteins after 1 mM H_2O_2 treatment. The 120-min sample was chosen for this analysis mainly because the greatest number of significantly changed transcript levels was detected at this time point based on microarray data. In total, 379 proteins were detected; among these proteins, nine were significantly increased and eighteen were significantly decreased (|Z score| > 2.0) when compared to the sample without H_2O_2 treatment.

Several proteins with increased abundance were interesting candidates for understanding the oxidative stress response. For instance, DVU0273, a conserved hypothetical protein predicted to be Fur-regulated, increased with Log_2R of 1.3 (Z=2.3), suggesting the regulatory role of Fur in oxidative stress. Possibly reflecting the damage of H_2O_2-generated ROS to the DNA molecule, DVU1078 a single-stranded nucleic acid binding R3H domain protein, had increased levels. Similarly, the increase in protein content of CysK (DVU 0663, cysteine synthase A) could be because the biosynthesis and /or repair of iron-sulfur cluster proteins were needed under oxidative stress (13). Sixteen out of the 18 proteins with significantly decreased levels were ribosomal proteins. Among those 16 ribosomal proteins, transcripts from five of their encoding genes were also found to be decreased. The slowdown of protein synthesis suggested by both proteomics and transcriptomics assays were in a good agreement with the temporary arrest of growth of the cells following the addition of 1 mM of H_2O_2.

However, in contrast to a total of 710 differentially transcribed genes detected with the same Z score cutoff, the protein response was much less. This disparity can be partially explained by the lack of correlation between gene expression and protein level changes at 120 min that yielded a Pearson correlation coefficient value of 0.072 (Table 1).

Predicted oxidative stress response genes. To gain a better, in-depth understanding of the molecular mechanisms of the *D. vulgaris* oxidative stress response, the microarray data were further examined according to the gene function groups. The detoxification system for ROS in aerobic and anaerobic bacteria has been reported to involve Sod, KatA and AhpC (2, 3, 20, 45). In addition, *D. vulgaris* has an alternative mechanism based on Rbo, Rbr and Rub to protect the cell against oxidative stress (13, 15, 41, 46). The transcript levels of these predicted oxidative stress response genes were examined. The expression of *sod* was not significantly changed and *katA* was significantly down-regulated ($\log_2$R=-1.95, -1.10 and -1.32 at 120, 240 and 480 min respectively), from which it was inferred that these two genes might not play major roles in detoxifying H_2O_2. In contrast, *ahpC*, *rdl* (homologue of *rub*) and *rbr2* (paralog of *rbr*) were increased more than three fold in transcript levels following peroxide treatment (Fig. 3). Increase of transcripts of *rbr* was less than two fold. The transcipts of *rub*, *rbo* and *ngr* (*rbr* homologue) were detected but their levels did not significantly change during this stress. Thus, AhpC, Rdl and Rbr2 appear to play important roles in detoxification of H_2O_2. Assuming that Rub/Rbr are needed, the baseline concentrations of these enzymes may be sufficient for meeting this oxidative stress.

PerR (DVU3095), a homologue of the peroxide-sensing regulator PerR in *B. subtilis*, is predicted to be involved in oxidative stress response (41). Therefore, the expression changes of the predicted PerR regulon genes were also investigated. With 1mM H_2O_2 treatment, not only

ahpC, *rdl, rbr2* and *rbr* as mentioned above, all other genes predicted to be in the *perR* regulon, *perR* and *DVU0772* were all significantly up-regulated (Fig. 3), which indicates that PerR has a regulatory role in response to oxidative stress as predicted.

Fur regulon. Fur, a paralog of PerR and regulator of iron homeostasis, has been shown to be important for bacterial growth and stress responses (2, 3, 20, 45). In the oxidative stress induced by H_2O_2, all of the predicted Fur regulon genes were up-regulated with *feoA-feoAB* and *genYZ* showing the highest up-regulation (Fig. 3). It is noted that the protein level of DVU0273 with the predicted strongest Fur binding site in the upstream of the gene (41), was also significantly increased (Table 1), which further supports the assumption that the major iron-uptake regulator Fur is involved in the H_2O_2-induced oxidative stress response.

Thioredoxin-dependent reduction systems. Thioredoxins are small ubiquitous proteins with a conserved Cys-Gly-Pro-Cys active site. Thioredoxins function as hydrogen donor for the reduction of a number of enzymes involved in DNA synthesis, protein repair and sulfur assimilation in addition to the direct or indirect reduction of H_2O_2 (47). With H_2O_2 treatment, thioredoxin reductase gene *trxB* was significantly up-regulated; thioredoxin *trx* and *DVU0725* encoding a thioredoxin domain containing hypothetical protein increased with a $\log_2$R of 1.52 and 1.75, respectively at 120 min; as expected, the expression of thiol-peroxidase *ahpC* was up-regulated as mentioned above; protein repair genes *msrAB* were significantly up-regulated as well (Table S2). These data strongly suggested the involvement of the thioredoxin-dependent systems in oxidative stress response.

Genes involved in DNA replication, recombination, and repair. In addition to the significantly increased expression of protein repair related genes mentioned above, some genes involved in DNA recombination and repair were also quickly and dramatically up-regulated

upon H_2O_2 treatment (Fig. 4). For instance, *radC* (*DVU1193*, a putative DNA repair protein) and *DVU0771* (a putative molybdenum-protein binding domain protein/site-specific recombinase, phage integrase) were detected to be induced with a $\log_2$R of 1.02, 1.38 and 2.36 for *radC*, and 1.33, 2.18 and 2.50 for *DVU0771* at 30, 60, and 120 min, respectively, which clustered in one clan. *DVU2907 (umuD)* was increased with a $\log_2$R of 1.87 and 1.75 at 30 and 60 min, respectively. *DVU2003* encoding a putative transposase was up-regulated with $\log_2$R of 2.00 and 2.75 at 60 and 120 min, respectively. The expression of *dcm* (*DVU1515*) encoding a putative type II DNA modification methyltransferase and *dnaG* (*DVU1789*) encoding a putative DNA primase were increased at 60, 120 and 480 min with $\log_2$R of 1.63, 2.41 and 2.17 for *dcm*, and 1.13, 1.96 and 1.06 for *dnaG*, which also clustered in one clan (Fig. 4). These results suggest the recruitment of DNA repair mechanisms for repair of DNA damage from H_2O_2 treatment.

Signal transduction mechanism genes. Two-component signal transduction is one of the mechanisms that bacteria use to sense and respond to the environment. *D. vulgaris* is in the upper 10% of bacteria in abundance of sensory histidine kinases (HK) and response regulators (RR) (48). *DVU3381* (*ntrC*) encoding a homolog of the transcriptional regulatory protein ZraR and *DVU3382* (*zraS*) encoding the apparent conjugate sensory protein are predicted to be in one operon. These two genes were among the most significantly up-regulated two-component signal transduction genes with H_2O_2 stress (Fig. 4). The $\log_2$R of these two genes were 1.32, 2.04, 2.86 and 2.08 for *DVU3381*, and 1.41, 2.34, 2.41 and 1.35 for *DVU3382* at 30, 60, 120 and 240 min, respectively. DVU3382 contains a PAS sensory domain which is suggested to be involved in sensing energy-related environmental factors such as oxygen, redox potential or light (43). The immediate and consistent up-regulation of *DVU3382* suggests that this sensory protein may play

a major role in sensing the redox potential in the cell, and that the response regulator DVU3381 may regulate its gene expression.

Besides the significant induction of two-component signal transduction system genes, expressions of several transcription regulators were significantly increased as well. For example, a predicted heat-inducible transcription repressor gene *hrcA*, an ArsR family transcriptional regulator gene *DVU1645* and a negative regulator of flagellin synthesis gene *flgM* were increased with $\log_2$R 1.51, 2.35 and 2.49 for *hrcA*, 1.11, 1.81 and 2.63 for *DVU1645*, and 1.01, 1.64 and 2.08 for *flgM*, respectively, at 30, 60 and 120 min (Fig. 4).

SRB signature genes. Genes involved in dissimilatory sulfate reduction pathways, oxidoreductase activities, and oxidative stress responses are considered to be characteristic of the SRB. There were 46 SRB genes in total identified by homology searches on four sulfate-reducing bacterial genomes, *D. vulgaris*, *D. alaskensis* G20, *Desulfotalea psychrophila*, and *Archaeoglobus fulgidus,* which are found uniquely when compared to 209 sequenced bacterial genomes available at the time of comparison (9). Microarray data from this study showed that most of the SRB signature genes, including *drsMKJOP*, *drsABC*, and *qmoABC*, were down-regulated (Fig. 4). Obviously, a general decrease in the sulfate reduction was consistent with decreased energy production, which also agreed with the slower growth under oxidative stress conditions.

Transcriptional and growth response of *ΔperR* and *Δfur* mutants to H_2O_2. Both transcriptomics and proteomics data suggest that PerR and Fur are involved in oxidative stress response. In order to further characterize the roles of PerR and Fur in H_2O_2-induced oxidative stress responses, transcriptional and growth response of both *ΔperR* and *Δfur* mutants to H_2O_2 were investigated.

Under standard growth conditions, as expected, the expression of *ahpC*, *rbr2* and *DVU0772,* which were preceded by a predicted PerR binding site, were de-repressed in *ΔperR* mutant. The expression of all Fur regulon genes except *DVU3123* was de-repressed in the *Δfur* mutant. In addition, the global regulator Fur was also observed negatively regulate 12 genes (*DVU2379-DVU2390*) downstream of *foxR* (a few genes with less than 3 fold increases were not shown in the table) (Table 2), which was consistent with gene expression data reported in Bender et al (4). With H_2O_2 stress, most of the de-repressed genes were not responsive in mutants. Interestingly, *ahpC* and *rbr2* were observed de-repressed in the mutant *Δfur* as well. By comparing the up-regulated stress response genes in wild-type *D. vulgaris* and mutants with de-repressed genes in deletion mutants *ΔperR* and *Δfur,* genes were de-repressed in mutant but not responsive under oxidative stress condition would be considered as PerR or Fur-dependent oxidative response genes. As shown in Table 2, in total, eight genes were Fur-dependent, two genes were PerR-dependent and five genes were PerR and Fur-dependent. Among these genes, Fur regulon genes such as *gdp*, *fld*, *genYZ(DVU0303-0304)*, *feoA-DVU2573-feoA* and Fur-de-repressed hypothetical gene *DVU2681* were Fur-dependent; Fur regulon genes *DVU0273*, *feoB,* Fur-depressed gene DVU2564 (*bioF*) and PerR regulon genes *ahpC*, *rbr2* were dependent on both PerR and Fur. PerR regulon gene *DVU0772* and a PerR-depressed hypothetical gene *DVU0024* were PerR-dependent. On the other hand, 33 genes were found up-regulated in both wild type and mutants *ΔperR* and *Δfur* when stress with H_2O_2 (Table 3), but not de-repressed in mutants *ΔperR* and *Δfur* (Table 2), which suggested that these genes were not regulated by either PerR or Fur in oxidative stress response.

When growth response to H_2O_2 was examined by monitoring the absorbance at 600 nm, largest OD change right after the addition of H_2O_2 was seen in *ΔperR*. However, the change of

final biomass yield according to OD readings in both *ΔperR* and *Δfur* were less than wild-type (Fig. 5), which suggested that the mutants were more resistant to H_2O_2 stress. Together with the transcriptional response, these results were inferred to mean that both PerR and Fur were involved in oxidative stress response by negatively regulating gene expression.

Conceptual cellular model of the oxidative stress response. To obtain further insights on the responses of *D. vulgaris* to oxidative stress, a conceptual cellular model was constructed based on the transcriptomic and proteomic data (Fig. 6). Increased cellular H_2O_2 had a dramatic effect on the gene expression, translation, and cell growth of *D. vulgaris.* Energy production and protein synthesis were slowed down and the cell growth was temporarily arrested. PerR and Fur regulons were detected with increased transcription levels and increased protein level for DVU0273, a predicted Fur regulon gene. The important roles of PerR and Fur in oxidative stress response were also demonstrated by the growth response of the *fur* and *perR* deletion mutants to the addition of H_2O_2. Transcript levels of *ΔperR* and *Δfur* mutants indicated that some H_2O_2 stress response genes were regulated by both PerR and Fur. An increased expression of genes involved in Rdl/Rbr2 and thioredoxin-dependent reduction pathways suggested their function in the defense against hydrogen peroxide. Protein and DNA repair genes and proteins were increased, while genes encoding energy production systems and sulfate reduction were decreased in transcription.

DISCUSSION

Given that anaerobic SRB such as *D. vulgaris* play a critical role in sulfur cycling, biocorrosion, and bioremediation of toxic metals, a better understanding of the oxidative stress responses in SRB is of great industrial and biological importance. These strict anaerobes exhibit

a remarkable level of aero-tolerance that likely contributes to their success in environmental settings. In this study, hydrogen peroxide was used to induce oxidative stress. Gene expression and protein content changes upon exposure to 1 mM of H_2O_2 were detected via transcriptomic and proteomic approaches. Comparisons of the wild-type and deletion mutants provided further evidence of gene regulation by PerR and Fur during oxidative stress. In addition, a gene co-expression network derived from the microarray data demonstrated possible interactions among genes involved in different gene functional categories, suggesting a complex set of genes are involved in the responses of *D. vulgaris* to H_2O_2.

Several lines of evidence support roles for PerR and Fur in regulating the oxidative stress response induced by hydrogen peroxide. First, the predicted PerR and Fur regulon genes (39) were significantly up-regulated followed the H_2O_2 treatment (Fig. 3). Second, protein levels of DVU0273, predicted to be Fur regulated, were also increased (Table 1). Third, both *ΔperR* and *Δfur* mutants were more resistant to H_2O_2 treatment than wild type (Fig. 5). The up-regulation of all predicted PerR and Fur regulon genes except *hdd(DVU3123)* and *foxR(DVU2378)* which were increased less than two fold during H_2O_2 induced stress was distinct. By examining other stress responses of *D. vulgaris*, we could determine whether the expression changes of the PerR and Fur regulated genes were unique to H_2O_2 exposure. The PerR regulon derepression was observed in *D. vulgaris* response to 0.1% O_2 exposure (36). In contrast, only a few Fur regulon genes were affected and those were down-regulated in response to a challenge with pure oxygen or air exposure (36, 38). Although increases in gene expression of all PerR regulon genes were found during heat shock, only *feoAB* and *gdp* were up-regulated in the Fur regulon (9). On the contrary, with exposure to nitrite, most of the Fur regulon genes were increased in transcription, while only the PerR-regulated *ahpC* was consistently up-regulated at 30-90 min. Therefore, it is

possible that these regulators may be involved in a common mechanism that *D. vulgaris* uses to cope with sub-lethal stresses.

Evidence from this study supports that Rdl and Rbr2 may be key enzymes for detoxification of hydrogen peroxide in *D. vulgaris*. H_2O_2 can be easily transformed into superoxide and hydroxyl radicals in the cell via enzymatic reactions. Therefore, to understand the enzymatic removal of cellular H_2O_2, both hydrogen peroxide scavenging enzymes and superoxide scavenging enzymes need to be considered. Superoxide scavenging enzyme genes *sod* and *rbo* were constitutively expressed based on raw hybridization signal intensities (data not shown) without significant changes. The gene encoding the H_2O_2 scavenging enzyme *katA* was significantly down-regulated, suggesting that catalase might not play a major role in the removal of H_2O_2. This might be expected since O_2 is generated in its reaction. Other H_2O_2 scavenging enzyme genes, such as *ngr* and *rub* were highly expressed based on raw signal intensities (data not shown), but they appeared not to respond specifically to H_2O_2 treatment. The change of *rbr* expression was less than two fold. Because *rdl* and *rbr2* were up-regulated in response to H_2O_2, they may be the key genes for H_2O_2 scavenging. This observation supports the assumption that Rbr homologues, Rbr2 or/and Ngr rather than Rbr (DVU3094) might confer H_2O_2 resistance, because no obvious oxidative stress phenotype was found for the *D. vulgaris rbr* mutant (15).

The oxidative stress resistance mechanism in *D. vulgaris* is distinctive. In *E. coli*, the oxidative stress response is regulated by a thiol switch in the regulator OxyR where a conformational change occurs through the formation of an intramolecular disulfide bond and activated OxyR protein stimulates transcription by direct contacting with RNA polymerase (42, 49). *B. subtilis* PerR senses H_2O_2 by metal-catalyzed oxidation (MCO) of a conserved histidine via the reaction between the bound ferrous ion and H_2O_2 (28). The oxidation of one of the

histidine ligands to iron (H37 or H91) is sufficient for the de-repression of the PerR regulon genes or other oxidative stress defense genes in an iron-containing medium. Two lines of evidences support that the oxidative stress response in *D. vulgaris* may differ from that of *B. subtilis* and *E. coli*. First, when *D. vulgaris* cells were subjected to H_2O_2, both PerR and Fur regulon genes were induced (Fig. 3) and most of them were regulated by both PerR and Fur (Table 2, 3); OxyR is the key regulator of the H_2O_2 stress response in *E. coli*; in *B. subtilis*, key transcription regulator PerR mediates both the response of its own gene and that of Fur (18). Also, in *D. vulgaris*, the up-regulated thioredoxin–dependent pathway was independent of PerR and Fur (Table 4); the *B. subtilis* PerR does not control genes involved in disulfide reduction (23, 25); in *E. coli*, the OxyR regulon includes genes involved in maintaining the intracellular thiols in the reduced states such as *gorA* (gluthathione reductase), *grxA* (glutaredoxin) and *trxA* (thioredoxin 2) (42, 49). However, the high similarity of protein sequences of *D. vulgaris* PerR and *B. subtilis* PerR and conserved amino acids which form the high-affinity Zn^{2+}-binding site (C96, C99, C136 and C139) and ligands for the regulatory ion, Fe^{2+} or Mn^{2+}(H37, D85, H91, H93 and D104) between these two proteins (Fig. S2) suggest that PerR in *D. vulgaris* may function as PerR in *B. subtilis*. Therefore, it will be very interesting to investigate whether *D. vulgaris* PerR is the key sensor for H_2O_2 stress and whether PerR regulon genes are de-repressed by MCO of PerR and identify any key regulators activated by the thiol switch in the future.

In summary, in response to increased cellular H_2O_2, the expression of genes (e.g., *rdl*/*rbr2*, *ahpC*) related to H_2O_2-scavenging and those genes encoding thioredoxin and thioredoxin reductase were up-regulated. An increased expression of the genes involved in protein repair, and DNA repair as well as genes for lipid metabolism were detected. Sulfate reduction and energy production systems were decreased and overall protein synthesis was slowed down,

consistent with the temporary growth inhibition caused by 1 mM H_2O_2. In addition, our analysis of gene expression changes in the Δ*fur* and Δ*perR* mutants of *D. vulgaris* demonstrated that the expression of *ahpC* and *rbr2* were regulated by both PerR and Fur. A comparison between oxidative stress responses of wild type *D. vulgaris* and the Δ*perR* and Δ*fur* mutants suggests that PerR and Fur may overlap in regulating gene expression in oxidative stress response. A further study of the function of PerR, Fur and other genes differentially expressed will allow us to better understand the roles of thiols and MCO systems in *D. vulgaris* responses to oxidative stress.

ACKNOWLEDGEMENTS

This work is part of the Environmental Stress Pathway Project (ESPP) of the Virtual Institute for Microbial Stress and Survival (http:://vimss.lbl.gov) supported by the U.S. Department of Energy, Office of Science, Office of Biological and Environmental research, Genomics: GTL Program through contract DE-AC02-05CH11231 with LBNL.

REFERENCES

1. **Alm, E. J., K. H. Huang, M. N. Price, R. P. Koche, K. Keller, I. L. Dubchak, and A. P. Arkin.** 2005. The MicrobesOnline web site for comparative genomics. Genome Res. **15:**1015-22.
2. **Andrews, S. C., A. K. Robinson, and F. Rodríguez-Quiñones.** 2003. Bacterial iron homeostasis. FEMS Microbiol. Rev.**27:**215-237.

3. **Bagg, A., and J. B. Neilands.** 1987. Ferric uptake regulation protein acts as a repressor, employing iron(II) as a cofactor to bind the operator of an iron transport operon in *Escherichia coli*. Biochemistry **26:**5471-5477.

4. **Bender, K. S., H.-C. B. Yen, C. L. Hemme, Z. Yang, Z. He, Q. He, J. Zhou, K. H. Huang, E. J. Alm, T. C. Hazen, A. P. Arkin, and J. D. Wall.** 2007. Analysis of a ferric uptake regulator (Fur) mutant of *Desulfovibrio vulgaris* Hildenborough. Appl. Environ. Microbiol. **73:**5389-5400.

5. **Bryant, D. W., D. R. McCalla, M. Leeksma, and P. Laneuville.** 1981. Type I nitroreductases of *Escherichia coli.* Can. J. Microbiol.**27:**81-86.

6. **Bsat, N., L. Chen, and J. D. Helmann.** 1996. Mutation of the *Bacillus subtilis* alkyl hydroperoxide reductase (ahpCF) operon reveals compensatory interactions among hydrogen peroxide stress genes. J. Bacteriol. **178:**6579-6586.

7. **Bsat, N., A. Herbig, L. Casillas-Martinez, P. Setlow, and J. D. Helmann.** 1998. *Bacillus subtilis* contains multiple Fur homologues: identification of the iron uptake (Fur) and peroxide regulon (PerR) repressors. Mol. Microbiol. **29:**189-198.

8. **Cabiscol, E., J. Tamarit, and J. Ros.** 2000. Oxidative stress in bacteria and protein damage by reactive oxygen species. Int. Microbiol. **3**:3-8.

9. **Chhabra, S. R., Q. He, K. H. Huang, S. P. Gaucher, E. J. Alm, Z. He, M. Z. Hadi, T. C. Hazen, J. D. Wall, J. Zhou, A. P. Arkin, and A. K. Singh.** 2006. Global analysis of heat shock response in *Desulfovibrio vulgaris* Hildenborough. J. Bacteriol. **188:**1817-1828.

10. **Clark, M. E., Q. He, Z. He, K. H. Huang, E. J. Alm, X. F. Wan, T. C. Hazen, A. P. Arkin, J. D. Wall, J. Z. Zhou, and M. W. Fields.** 2006. Temporal transcriptomic

analysis as *Desulfovibrio vulgaris* Hildenborough transitions into stationary phase during electron donor depletion. Appl. Environ. Microbiol. **72:**5578-5588.

11. **Clauset, A., M. E. Newman, and C. Moore.** 2004. Finding community structure in very large networks. Phys. Rev. E Stat. Nonlin. Soft Matter Phys. **70:**066111.

12. **Eisen, M. B., P. T. Spellman, P. O. Brown, and D. Botstein.** 1998. Cluster analysis and display of genome-wide expression patterns. Proc. Natl. Acad. Sci. USA **95:**14863–14868.

13. **Fournier, M., C. Aubert, Z. Dermoun, M.-C. Durand, D. Moinier, and A. Dolla.** 2006. Response of the anaerobe *Desulfovibrio vulgaris* Hildenborough to oxidative conditions: proteome and transcript analysis. Biochimie **88:**85-94.

14. **Fournier, M., Z. Dermoun, M.-C. Durand, and A. Dolla.** 2004. A new function of the *Desulfovibrio vulgaris* Hildenborough [Fe] hydrogenase in the protection against oxidative stress. J. Biol. Chem. **279:**1787-1793.

15. **Fournier, M., Y. Zhang, J. D. Wildschut, A. Dolla, J. K. Voordouw, D. C. Schriemer, and G. Voordouw.** 2003. Function of oxygen resistance proteins in the anaerobic, sulfate-reducing bacterium *Desulfovibrio vulgaris* Hildenborough. J. Bacteriol. **185:**71-79.

16. **Fridovich, I.** 1978. The biology of oxygen radicals. Science **201:**875-880.

17. **Fuangthong, M., S. Atichartpongkul, S. Mongkolsuk, and J. D. Helmann.** 2001. OhrR is a repressor of ohrA, a key organic hydroperoxide resistance determinant in *Bacillus subtilis*. J. Bacteriol. **183:**4134-4141.

18. **Fuangthong, M., A. F. Herbig, N. Bsat, and J. D. Helmann.** 2002. Regulation of the *Bacillus subtilis* fur and perR Genes by PerR: not all members of the PerR regulon are peroxide inducible. J. Bacteriol. **184:**3276-3286.

19. **Gaballa, A., and J. D. Helmann.** 2002. A peroxide-induced zinc uptake system plays an important role in protection against oxidative stress in *Bacillus subtilis*. Mol. Microbiol. **45:**997 - 1005.

20. **Hassett, D., P. Sokol, M. Howell, and M. Vasil.** 1996. Ferric uptake regulator (Fur) mutants of *Pseudomonas aeruginosa* demonstrate defective siderophore-mediated iron uptake, altered aerobic growth, and decreased superoxide dismutase and catalase activities. J. Bacteriol. **178:**3996-4003.

21. **He, Q., K. H. Huang, Z. He, E. J. Alm, M. W. Fields, T. C. Hazen, A. P. Arkin, J. D. Wall, and J. Zhou.** 2006. Energetic consequences of nitrite stress in *Desulfovibrio vulgaris* Hildenborough, inferred from global transcriptional analysis. Appl. Environ. Microbiol. **72:**4370-4381.

22. **Heidelberg, J. F., R. Seshadri, S. A. Haveman, C. L. Hemme, I. T. Paulsen, J. F. Kolonay, J. A. Eisen, N. Ward, B. Methe, L. M. Brinkac, S. C. Daugherty, R. T. Deboy, R. J. Dodson, A. S. Durkin, R. Madupu, W. C. Nelson, S. A. Sullivan, D. Fouts, D. H. Haft, J. Selengut, J. D. Peterson, T. M. Davidsen, N. Zafar, L. Zhou, D. Radune, G. Dimitrov, M. Hance, K. Tran, H. Khouri, J. Gill, T. R. Utterback, T. V. Feldblyum, J. D. Wall, G. Voordouw, and C. M. Fraser.** 2004. The genome sequence of the anaerobic, sulfate-reducing bacterium *Desulfovibrio vulgaris* Hildenborough. Nat. Biotech. **22:**554-559.

23. **Helmann, J. D., M. F. W. Wu, A. Gaballa, P. A. Kobel, M. M. Morshedi, P. Fawcett, and C. Paddon.** 2003. The global transcriptional response of *Bacillus subtilis* to peroxide stress is coordinated by three transcription factors. J. Bacteriol. **185:**243-253.

24. **Horsburgh, M. J., M. O. Clements, H. Crossley, E. Ingham, and S. J. Foster.** 2001. PerR controls oxidative stress resistance and iron storage proteins and is required for virulence in *Staphylococcus aureus*. Infect. Immun. **69:**3744-3754.

25. **Imlay, J. A.** 2008. Cellular defenses against superoxide and hydrogen peroxide. Annu. Rev. Biochem. **77:**755-776.

26. **Jenney Jr., F. E., M. F. J. M. Verhagen, X. Cui, and M. W. W. Adams.** 1999. Anaerobic microbes: oxygen detoxification without superoxide dismutase. Science **286:**306-309.

27. **Johnson, M. S., I. B. Zhulin, M. E. Gapuzan, and B. L. Taylor.** 1997. Oxygen-dependent growth of the obligate anaerobe *Desulfovibrio vulgaris* Hildenborough. J. Bacteriol. **179:**5598-5601.

28. **Lee, J.-W., and J. D. Helmann.** 2006. The PerR transcription factor senses H_2O_2 by metal-catalysed histidine oxidation. Nature **440:**363-367.

29. **Liochev, S. I., A. Hausladen, and I. Fridovich.** 1999. Nitroreductase A is regulated as a member of the soxRS regulon of *Escherichia coli*. Proc. Natl. Acad. Sci. USA **96:**3537-3539.

30. **Lobo, S. A., A. M. Melo, J. N. Carita, M. Teixeira, and L. M. Saraiva.** 2007. The anaerobe *Desulfovibrio desulfuricans* ATCC 27774 grows at nearly atmospheric oxygen levels. FEBS Lett. **581:**433-6.

31. **Lumppio, H. L., N. V. Shenvi, A. O. Summers, G. Voordouw, and D. M. Kurtz, Jr.** 2001. Rubrerythrin and rubredoxin oxidoreductase in *Desulfovibrio vulgaris*: a novel oxidative stress protection system. J. Bacteriol. **183:**101-108.

32. **Luo, F., Y. Yang, J. Zhong, H. Gao, L. Khan, D. Thompson, and J. Zhou.** 2007. Constructing gene co-expression networks and predicting functions of unknown genes by random matrix theory. BMC Bioinformatics **8:**299.

33. **Miller, R. A., and B. E. Britigan.** 1997. Role of oxidants in microbial pathophysiology. Clin. Microbiol. Rev. **10:**1-18.

34. **Mostertz, J., C. Scharf, M. Hecker, and G. Homuth.** 2004. Transcriptome and proteome analysis of *Bacillus subtilis* gene expression in response to superoxide and peroxide stress. Microbiology **150:**497-512.

35. **Mukhopadhyay, A., Z. He, E. J. Alm, A. P. Arkin, E. E. Baidoo, S. C. Borglin, W. Chen, T. C. Hazen, Q. He, H.-Y. Holman, K. Huang, R. Huang, D. C. Joyner, N. Katz, M. Keller, P. Oeller, A. Redding, J. Sun, J. Wall, J. Wei, Z. Yang, H.-C. Yen, J. Zhou, and J. D. Keasling.** 2006. Salt stress in *Desulfovibrio vulgaris* Hildenborough: an integrated genomics approach. J. Bacteriol. **188:**4068-4078.

36. **Mukhopadhyay, A., A. M. Redding, M. P. Joachimiak, A. P. Arkin, S. E. Borglin, P. S. Dehal, R. Chakraborty, J. T. Geller, T. C. Hazen, Q. He, D. C. Joyner, V. J. J. Martin, J. D. Wall, Z. K. Yang, J. Zhou, and J. D. Keasling.** 2007. Cell-wide responses to low-oxygen exposure in *Desulfovibrio vulgaris* Hildenborough. J. Bacteriol. **189:**5996-6010.

37. **Newman, M. E.** 2006. Modularity and community structure in networks. Proc Natl Acad Sci USA **103:**8577-82.

38. **Pereira, P., Q. He, A. Xavier, J. Zhou, I. Pereira, and R. Louro.** 2008. Transcriptional response of *Desulfovibrio vulgaris* Hildenborough to oxidative stress mimicking environmental conditions. Arch. Microbiol. **189:**451-461.

39. **Rea, R., C. Hill, and C. G. M. Gahan.** 2005. *Listeria monocytogenes* perR mutants display a small-colony phenotype, increased sensitivity to hydrogen peroxide, and significantly reduced murine virulence. Appl. Environ. Microbiol. **71:**8314-8322.

40. **Redding, A. M., A. Mukhopadhyay, D. C. Joyner, T. C. Hazen, and J. D. Keasling.** 2006. Study of nitrate stress in *Desulfovibrio vulgaris* Hildenborough using iTRAQ proteomics. Brief. Funct. Genomic Proteomic **5:**133-143.

41. **Rodionov, D., I. Dubchak, A. Arkin, E. Alm, and M. Gelfand.** 2004. Reconstruction of regulatory and metabolic pathways in metal-reducing delta-proteobacteria. Genome Biology **5:**R90.

42. **Tao, K., N. Fujita, and A. Ishihama.** 1993. Involvement of the RNA polymerase α subunit C-terminal region in co-operative interaction and transcriptional activation with OxyR protein. Mol. Microbiol. **7:**859-864.

43. **Taylor, B. L., and I. B. Zhulin.** 1999 PAS Domains: Internal Sensors of Oxygen, Redox Potential, and Light. Microbiol. Mol. Biol. Rev. **63:**479–506.

44. **Thompson, D. K., A. S. Beliaev, C. S. Giometti, S. L. Tollaksen, T. Khare, D. P. Lies, K. H. Nealson, H. Lim, J. Yates, III, C. C. Brandt, J. M. Tiedje, and J. Zhou.** 2002. Transcriptional and proteomic analysis of a ferric uptake regulator (Fur) mutant of *Shewanella oneidensis*: possible involvement of Fur in energy metabolism, transcriptional regulation, and oxidative stress. Appl. Environ. Microbiol. **68:**881-892.

45. **Touati, D., M. Jacques, B. Tardat, L. Bouchard, and S. Despied.** 1995. Lethal oxidative damage and mutagenesis are generated by iron in delta fur mutants of *Escherichia coli*: protective role of superoxide dismutase. J. Bacteriol. **177:**2305-2314.

46. **Wildschut, J. D., R. M. Lang, J. K. Voordouw, and G. Voordouw.** 2006. Rubredoxin:oxygen oxidoreductase enhances survival of *Desulfovibrio vulgaris* Hildenborough under microaerophilic conditions. J. Bacteriol. **188:**6253-6260.

47. **Zeller, T., and G. Klug.** 2006. Thioredoxins in bacteria: functions in oxidative stress response and regulation of thioredoxin genes. Naturwissenschaften **93:**259-266.

48. **Zhang, W., D. Culley, M. Hogan, L. Vitiritti, and F. Brockman.** 2006. Oxidative stress and heat-shock responses in *Desulfovibrio vulgaris* by genome-wide transcriptomic analysis. Antonie Leeuwenhoek **90:**41-55.

49. **Zheng, M., X. Wang, L. J. Templeton, D. R. Smulski, R. A. LaRossa, and G. Storz.** 2001. DNA microarray-mediated transcriptional profiling of the *Escherichia coli* response to hydrogen peroxide. J. Bacteriol. **183:**4562-4570.

50. **Zhou, J., M. A. Bruns, and J. M. Tiedje.** 1996. DNA recovery from soils of diverse composition. Appl. Environ. Microbiol. **62:**316-22.

Figure Legends

FIG. 1. Growth response of *D. vulgaris* to 1 mM H_2O_2 treatment and the temporal profiling of the transcriptomic response. (A) Growth response of *D. vulgaris* was monitored as changes in OD_{600}. Dark red symbols: control culture, water was added; dark cyan symbols: treatment cultures, 1 mM H_2O_2 was added. Arrow indicates the time of additions. Growth of 2 hrs before and 8 hrs after the addition of H_2O_2 was shown in the insert. B) Numbers of genes differentially transcribed following addition of 1 mM H_2O_2 ($|Log_2R$ (treatment/control)$|>1$, $|Z| >1.5$). Positive and negative numbers indicate number of genes with increased and decreased levels of transcription in the experimental cultures versus the control, respectively. C) Detrended Correspondence Analysis (DCA) of the transcriptional changes. Overall similarity of the microarray gene expression profiles for H_2O_2-treated and control samples among the different time points was determined by DCA analysis.

FIG. 2. Gene co-expression network from the H_2O_2 stress microarray profiles generated by the random matrix theory approach. Modules with more than four genes were shown. Annotations for genes identified by DVU numbers can be found at Microbes Online (http://www.microbesonline.org/). Each node represents a gene. Blue and gray lines indicate positive and negative correlation coefficients, respectively. Colors were assigned to nodes according to their gene function categories: red, energy production and conversion; yellow, posttranslational modification, protein turnover, chaperons; green, DNA replication, recombination and repair; purple, signal transduction mechanisms; brown, lipid transport and metabolism; green, yellow-carbohydrate, amino acid or nucleotide transport and metabolism; magenta-translation, ribosomal structure and biogenesis; pink, cell envelope, biogenesis, outer membrane; light cyan, transcription; orange, secondary metabolite biosynthesis, transport and

catabolism; dark cyan, coenzyme transport and metabolism; tan, intracellular trafficking, secretion and vesicular transport; salmon, cell cycle control, cell division and chromosome partitioning; grey, defense mechanisms; dark grey, general function prediction; white, function unknown.

FIG. 3. Expression profiling of predicted PerR (A) and Fur regulons (B) across the time course. *predicated binding site found in the upstream of the gene or operon.

FIG. 4. Gene expression profiles of selected genes. A, Genes involved in DNA replication, recombination and repair. B. Genes involved in signal transduction mechanisms. C. SRB signature genes.

FIG. 5. Growth responses of wild type *D. vulgaris* and deletion mutants *fur* (JW707) and *perR* (JW708) to H_2O_2 treatment. Arrows indicates the time points when H_2O_2 or water was added in the culture.

FIG. 6. A conceptual cellular model of the response of *D. vulgaris* Hildenborough to 1 mM H_2O_2. Orange and green indicate increased or decreased gene expression respectively; blue represents genes without significant expression changes. The transcriptional regulators were marked with star and purple indicates increased gene expression level. The detoxification likely results from increased expression of the genes for Rdl/Rbr2 and the thioredoxin-dependent reduction pathway. Genes for sulfate reduction were decreased, while those encoding enzymes for the oxidation of lactate through pyruvate, acetyl-CoA and formate were increased. The increased cellular H_2O_2 appear to have resulted in an increased iron influx, protein and DNA repair response. The complexity of the gene regulation was shown by the up-regulation of several transcriptional regulators.

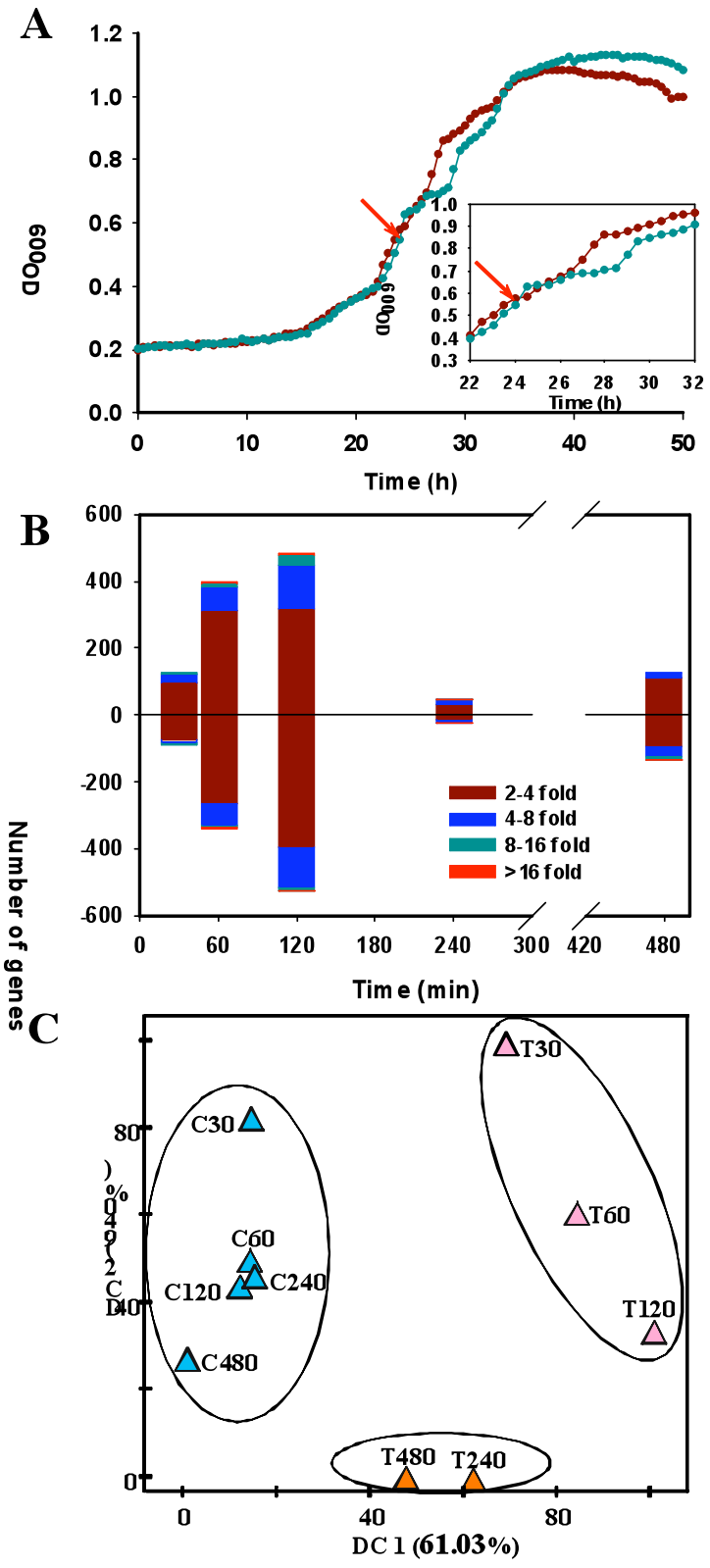
A
1.2
1.0
0.8
0.6
0.4
0.2
0.0
OD600
0
10
20
30
40
50
Time (h)
1.0
0.9
0.8
0.7
0.6
0.5
0.4
0.3
22
24
26
28
30
32
Time (h)
B
600
400
200
0
-200
-400
-600
Number of genes
0
60
120
180
240
300
420
480
Time (min)
2-4 fold
4-8 fold
8-16 fold
>16 fold
C
T30
C30
80
T60
C60
C120
C240
T120
C480
T480
T240
0
40
80
DC 1 (61.03%)

Figure 1

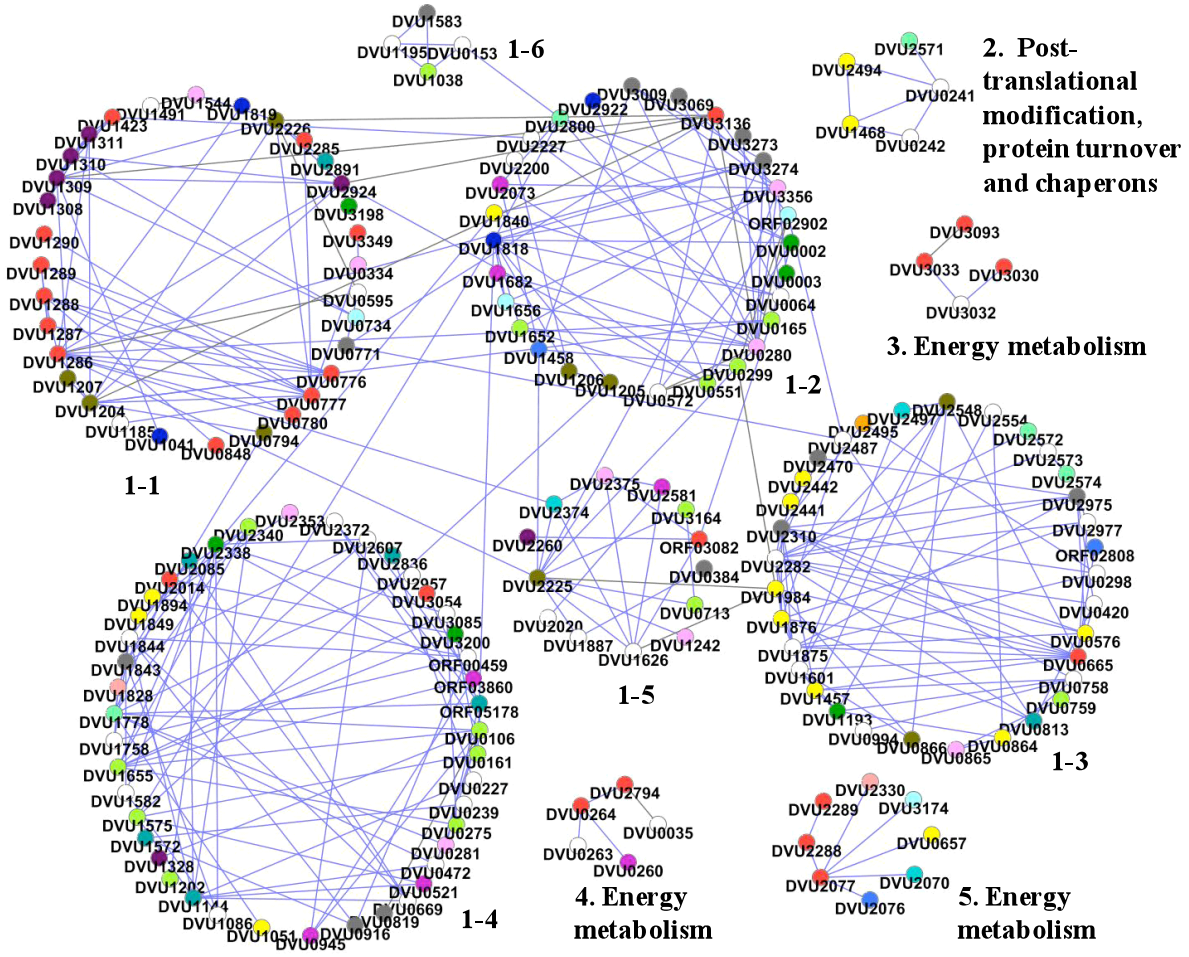
1-6
2. Post-translational modification, protein turnover and chaperons
3. Energy metabolism
1-2
1-1
1-5
1-3
1-4
4. Energy metabolism
5. Energy metabolism

Figure 2

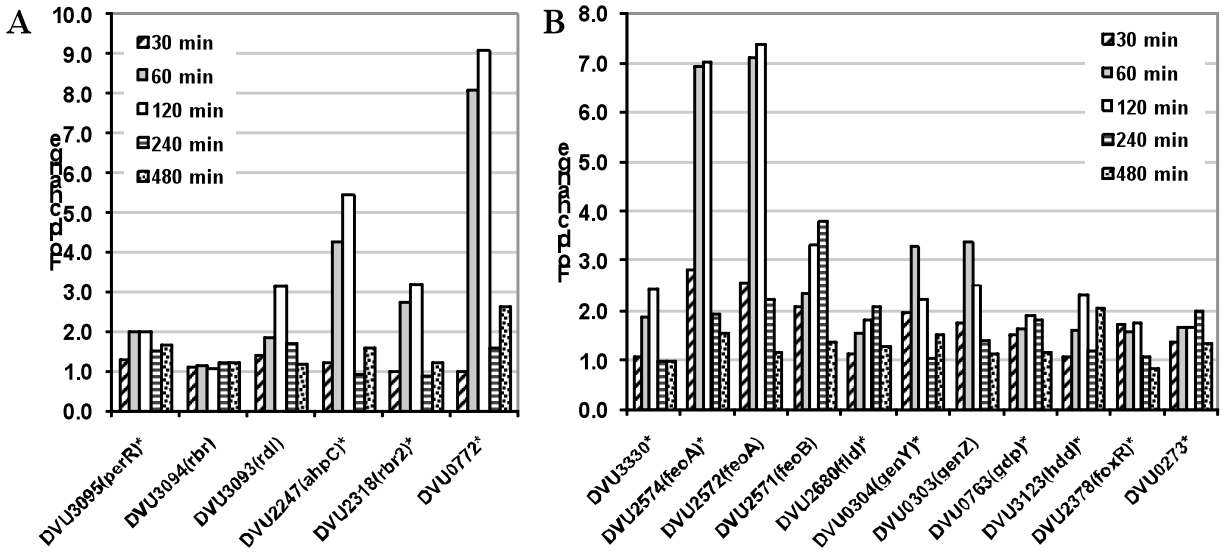
A
B
30 min
60 min
120 min
240 min
480 min
DVU3095(perR)*
DVU3094(rbr)
DVU3093(rdl)
DVU2247(ahpC)*
DVU2318(rbr2)*
DVU0772*
DVU3330*
DVU2574(feoA)*
DVU2572(feoA)
DVU2571(feoB)
DVU2680(fld)*
DVU0304(genY)*
DVU0303(genZ)
DVU0763(gdp)*
DVU3123(hddl)*
DVU2378(foxR)*
DVU0273*

Figure 3

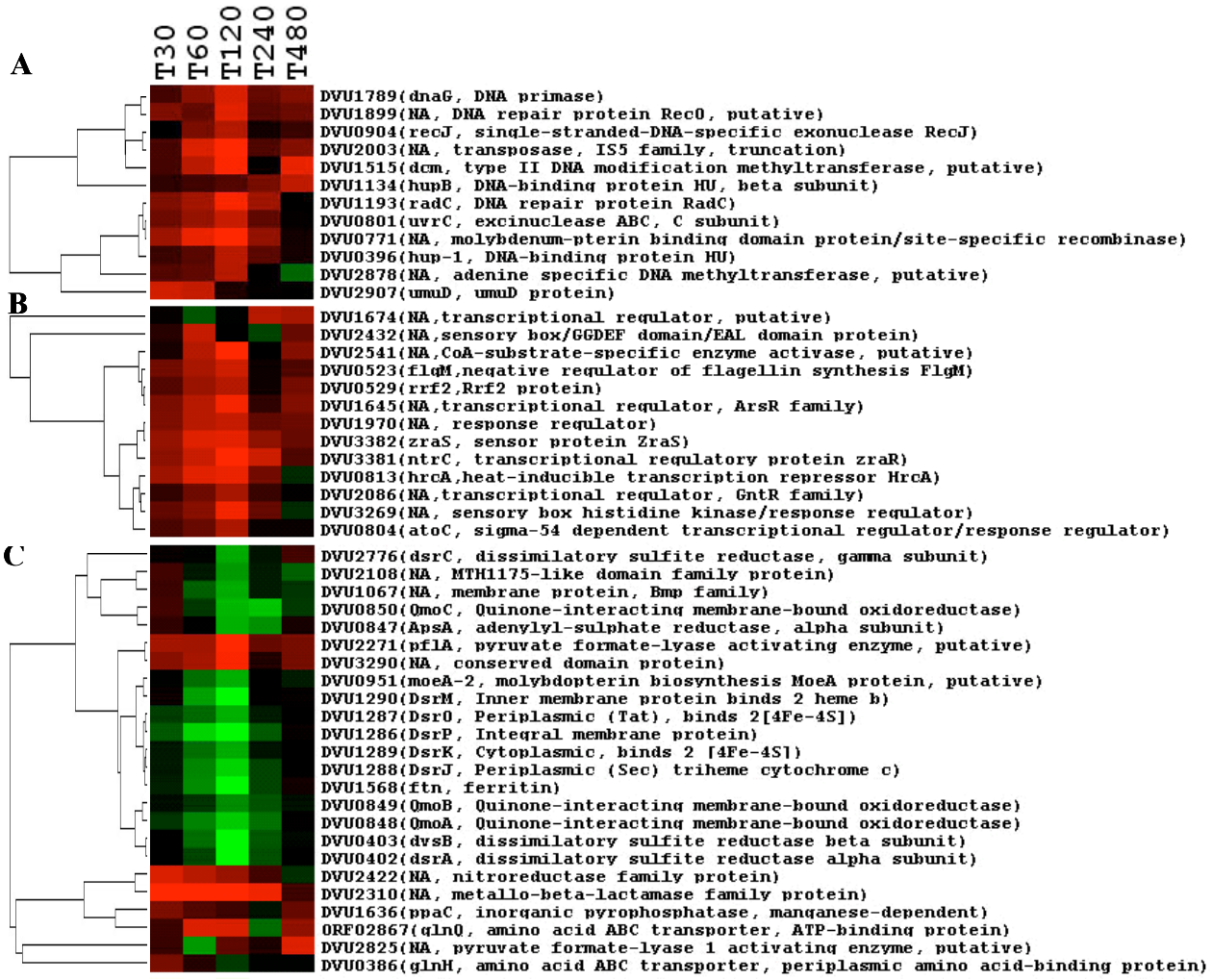
T30
T60
T120
T240
T480
A
DVU1789(dnaG, DNA primase)
DVU1899(NA, DNA repair protein RecO, putative)
DVU0904(recJ, single-stranded-DNA-specific exonuclease RecJ)
DVU2003(NA, transposase, IS5 family, truncation)
DVU1515(dcm, type II DNA modification methyltransferase, putative)
DVU1134(hupB, DNA-binding protein HU, beta subunit)
DVU1193(radC, DNA repair protein RadC)
DVU0801(uvrC, excinuclease ABC, C subunit)
DVU0771(NA, molybdenum-pterin binding domain protein/site-specific recombinase)
DVU0396(hup-1, DNA-binding protein HU)
DVU2878(NA, adenine specific DNA methyltransferase, putative)
DVU2907(umuD, umuD protein)
B
DVU1674(NA,transcriptional regulator, putative)
DVU2432(NA,sensory box/GGDEF domain/EAL domain protein)
DVU2541(NA,CoA-substrate-specific enzyme activase, putative)
DVU0523(flgM,negative regulator of flagellin synthesis FlgM)
DVU0529(rrf2,Rrf2 protein)
DVU1645(NA,transcriptional regulator, ArsR family)
DVU1970(NA, response regulator)
DVU3382(zraS, sensor protein ZraS)
DVU3381(ntrC, transcriptional regulatory protein zraR)
DVU0813(hrcA,heat-inducible transcription repressor HrcA)
DVU2086(NA,transcriptional regulator, GntR family)
DVU3269(NA, sensory box histidine kinase/response regulator)
DVU0804(atoC, sigma-54 dependent transcriptional regulator/response regulator)
C
DVU2776(dsrC, dissimilatory sulfite reductase, gamma subunit)
DVU2108(NA, MTH1175-like domain family protein)
DVU1067(NA, membrane protein, Bmp family)
DVU0850(QmoC, Quinone-interacting membrane-bound oxidoreductase)
DVU0847(ApsA, adenylyl-sulphate reductase, alpha subunit)
DVU2271(pflA, pyruvate formate-lyase activating enzyme, putative)
DVU3290(NA, conserved domain protein)
DVU0951(moeA-2, molybdopterin biosynthesis MoeA protein, putative)
DVU1290(DsrM, Inner membrane protein binds 2 heme b)
DVU1287(DsrO, Periplasmic (Tat), binds 2[4Fe-4S])
DVU1286(DsrP, Integral membrane protein)
DVU1289(DsrK, Cytoplasmic, binds 2 [4Fe-4S])
DVU1288(DsrJ, Periplasmic (Sec) triheme cytochrome c)
DVU1568(ftn, ferritin)
DVU0849(QmoB, Quinone-interacting membrane-bound oxidoreductase)
DVU0848(QmoA, Quinone-interacting membrane-bound oxidoreductase)
DVU0403(dvsB, dissimilatory sulfite reductase beta subunit)
DVU0402(dsrA, dissimilatory sulfite reductase alpha subunit)
DVU2422(NA, nitroreductase family protein)
DVU2310(NA, metallo-beta-lactamase family protein)
DVU1636(ppaC, inorganic pyrophosphatase, manganese-dependent)
ORF02867(glnQ, amino acid ABC transporter, ATP-binding protein)
DVU2825(NA, pyruvate formate-lyase 1 activating enzyme, putative)
DVU0386(glnH, amino acid ABC transporter, periplasmic amino acid-binding protein)

Figure 4

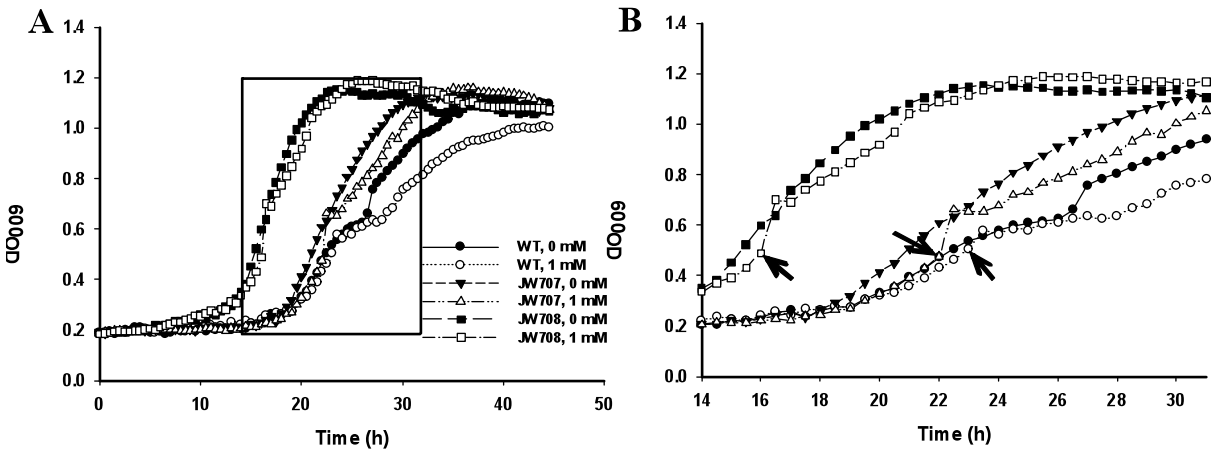
A
B
OD600
Time (h)
WT, 0 mM
WT, 1 mM
JW707, 0 mM
JW707, 1 mM
JW708, 0 mM
JW708, 1 mM

Figure 5

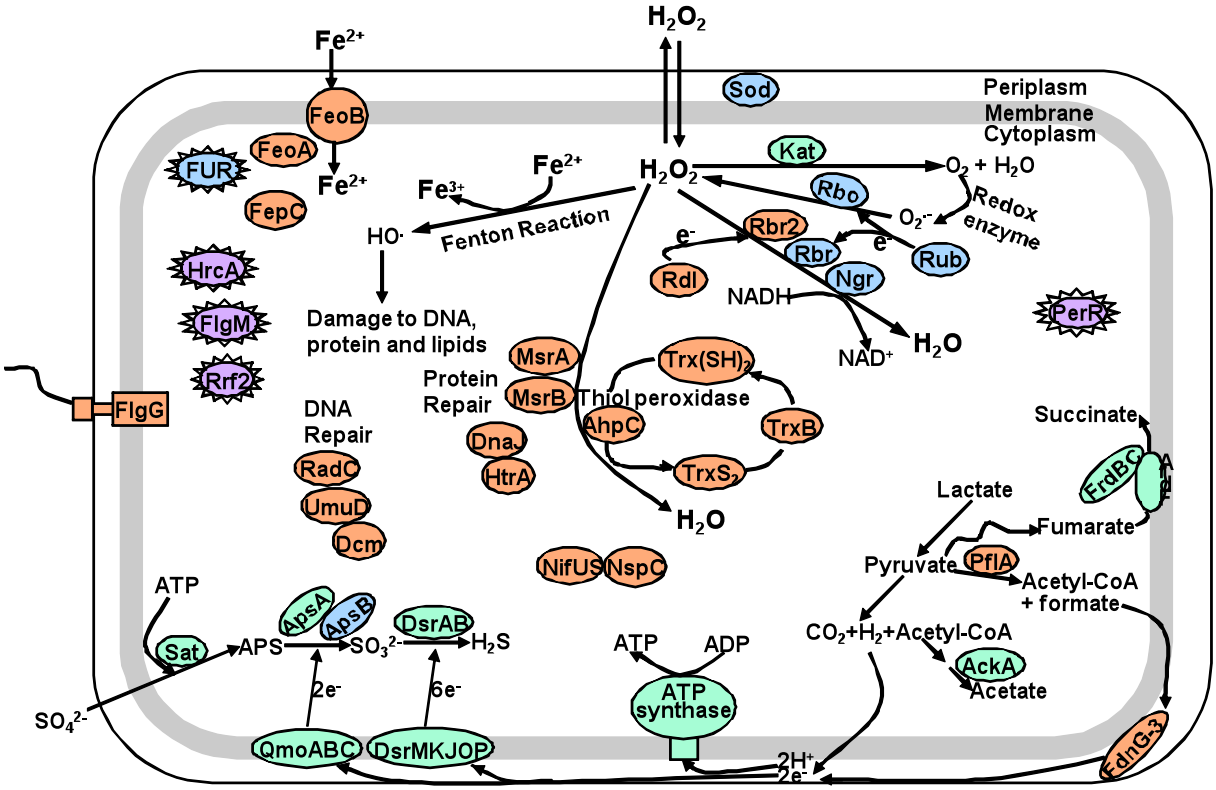
H_2O_2
Fe^{2+}
FeoB
FeoA
FUR
FepC
Fe^{2+}
Fe^{3+}
Fe^{2+}
HO·
Fenton Reaction
Damage to DNA, protein and lipids
HrcA
FlgM
Rrf2
FlgG
DNA Repair
RadC
UmuD
Dcm
Protein Repair
MsrA
MsrB
DnaJ
HtrA
Sod
Periplasm
Membrane
Cytoplasm
Kat
$O_2 + H_2O$
Rbo
$O_2^{\cdot-}$
Redox enzyme
Rbr2
Rbr
Rub
Ngr
Rdl
e-
e-
NADH
NAD^+
H_2O
PerR
Thiol peroxidase
$Trx(SH)_2$
AhpC
TrxB
$TrxS_2$
H_2O
NifUS
NspC
Succinate
FrdBC
Lactate
Fumarate
Pyruvate
PflA
Acetyl-CoA + formate
CO_2+H_2+Acetyl-CoA
AckA
Acetate
ATP
Sat
APS
ApsA
ApsB
SO_3^{2-}
DsrAB
H_2S
SO_4^{2-}
2e-
6e-
QmoABC
DsrMKJOP
ATP
ADP
ATP synthase
$2H^+$
$2e^-$
F-dnG-3

Figure 6

TABLE 1. Microarray and proteomics data for proteins with the most significant differential level in response to 1 mM H_2O_2

DVU no.	Name	Annotated function	Microarray Log_2 R					iTRAQ Log_2 R
			30 min	60 min	120 min	240 min	480 min	120 min
DVU0799	NA	conserved hypothetical protein	NA	NA	-1.5(-0.0)	NA	NA	2.3(4.2)
DVU1375	NA	hypothetical protein	0.2(0.4)	-0.3(-0.5)	-0.9(-1.4)	-0.3(-0.5)	-0.3(-0.6)	1.3(2.4)
DVU3199	NA	TIGR00103	NA	-0.6(-1.1)	-1.0(-1.9)	0.1(0.1)	-0.0(-0.1)	1.3(2.4)
DVU0273	NA	conserved hypothetical protein	0.5(0.9)	0.7(1.4)	0.8(1.4)	1.0(1.0)	0.4(0.8)	1.3(2.3)
DVU0797	NA	conserved hypothetical protein	NA	NA	NA	NA	NA	1.1(2.0)
DVU0508	infB	translation initiation factor IF-2	-0.4(-0.7)	-0.4(-0.8)	-0.2(-0.4)	0.2(0.3)	0.4(0.8)	1.1(2.0)
DVU1265	NA	hypothetical protein	1.0(1.8)	1.2(2.1)	**1.5(2.0)**	-0.0(-0.0)	0.4(0.7)	**1.1(2.0)**
DVU0663	cysK	cysteine synthase A	0.1(0.2)	0.2(0.3)	0.5(0.9)	0.5(0.5)	-0.3(-0.5)	1.1(2.0)
DVU1078	NA	R3H domain protein	-0.6(-0.0)	NA	-0.2(-0.0)	-0.1(-0.1)	0.8(1.4)	1.2(2.2)
DVU1326	rpsM	ribosomal protein S13	-0.4(-0.8)	-0.8(-1.5)	**-1.0(-2.0)**	0.0(0.0)	0.2(0.4)	**-1.3(-2.1)**
ORFA00060	NA	transcriptional regulator, AbrB family	NA	NA	NA	NA	NA	-1.5(-2.4)
DVU1303	rplC	ribosomal protein L3	-0.2(-0.3)	-0.5(-1.0)	**-1.0(-1.8)**	0.0(0.0)	0.1(0.2)	**-1.3(-2.2)**
DVU1304	rplD	ribosomal protein L4	-0.0(-0.1)	-0.2(-0.3)	-0.6(-1.0)	-0.2(-0.4)	0.1(0.1)	-1.3(-2.2)
DVU1318	rplF	ribosomal protein L6	-0.0(-0.1)	-0.3(-0.5)	**-1.0(-1.6)**	-0.1(-0.2)	0.3(0.6)	**-1.3(-2.2)**
DVU2518	rplM	ribosomal protein L13	-0.3(-0.5)	-0.6(-1.1)	**-1.3(-2.4)**	0.2(0.3)	0.2(0.4)	**-2.0(-3.3)**
DVU1310	rplP	ribosomal protein L16	-0.4(-0.8)	-1.0(-1.9)	**-1.6(-2.9)**	-0.2(-0.4)	-0.0(-0.0)	**-1.4(-2.3)**
DVU1330	rplQ	ribosomal protein L17	-0.2(-0.5)	-0.5(-1.1)	-0.8(-1.4)	0.2(0.4)	0.2(0.4)	-1.3(-2.1)
DVU1319	rplR	ribosomal protein L18	-0.1(-0.2)	-0.2(-0.4)	-0.6(-1.0)	-0.2(-0.3)	0.2(0.3)	-2.0(-3.3)
DVU0835	rplS	ribosomal protein L19	0.6(1.1)	0.2(0.4)	0.2(0.4)	0.4(0.7)	0.4(0.8)	-2.0(-3.3)
DVU1314	rplX	ribosomal protein L24	0.0(0.1)	-0.6(-1.0)	-0.5(-0.8)	0.1(0.2)	-0.1(-0.1)	-1.8(-3.1)
DVU1211	rpmB	ribosomal protein L28	-0.3(-0.0)	-0.7(-1.2)	-0.2(-0.3)	0.6(1.1)	0.6(1.1)	-2.6(-4.4)
DVU2519	rpsI	ribosomal protein S9	NA	0.2(0.0)	0.1(0.2)	0.0(0.0)	0.4(0.8)	-2.0(-3.3)
DVU1327	rpsK	ribosomal protein S11	-0.5(-0.9)	-0.4(-0.7)	-0.7(-1.2)	-0.1(-0.2)	0.3(0.6)	-1.4(-2.4)
DVU0504	rpsO	ribosomal protein S15	0.0(0.1)	0.3(0.6)	0.5(0.9)	1.2(2.0)	0.8(1.4)	-1.9(-3.1)
DVU0839	rpsP	ribosomal protein S16	-0.0(-0.0)	-0.1(-0.2)	-0.4(-0.8)	0.1(0.1)	0.7(1.3)	-1.6(-2.6)
DVU1298	rpsL	ribosomal protein S12	NA	NA	-0.4(-0.7)	0.2(0.3)	NA	-1.9(-3.1)
DVU2091	thiE-1	thiamine-phosphate pyrophosphorylase	-0.1(-0.2)	0.1(0.3)	0.3(0.4)	0.2(0.3)	-0.3(-0.5)	-3.2(-5.5)

R: treatment/control. Values in parentheses are z scores.

Boldface indicates more than two folds of change ($|Log2R| \geq 1$) in both transcript and protein level.

TABLE 2. Selected transcriptomics data in deletion mutants Δfur and ΔperR under standard growth condition and H_2O_2 stress

			De-repression of genes		Response to H_2O_2 in strain		
			No stress		1 mM H_2O, 120 min vs 0 mM, 120 min		
DVU no.	Name	Annotated function	Δfur/WT	ΔperR/WT	Δfur	ΔperR	WT
DVU0763[a]*	gdp	GGDEF domain protein	**4.5**	-0.5	-0.6	1.2	**1.7**
DVU2377		hypothetical protein	**2.3**	0.3	-0.3	0.6	0.7
DVU2378[a]	foxR	transcriptional regulator, AraC family	**3.3**	0.0	-0.1	0.1	0.8
DVU2379	pqqL	peptidase, M16 family, putative	**2.3**	-0.6	-0.3	0.4	0.4
DVU2380	atpX	ABC transporter, ATP-binding protein	**2.7**	0.4	-1.4	-0.1	1.0
DVU2381		conserved hypothetical protein	**4.6**	-0.2	-1.1	0.2	0.7
DVU2383		tonB dependent receptor domain protein	**5.0**	-0.3	-1.2	-0.2	-0.1
DVU2384		ABC transporter, periplasmic substrate-binding protein	**1.8**	0.1	-0.4	0.3	1.1
DVU2388	tolQ-1	tolQ protein	**2.0**	0.1	-0.3	-0.3	0.5
DVU2389	tolR	biopolymer transport protein, ExbD/TolR family	**1.7**	0.3	-0.6	0.6	0.8
DVU2390		TonB domain protein	**1.6**	-0.2	-0.6	0.5	0.5
DVU2456		hypothetical protein	**1.8**	1.1	-0.2	-0.5	0.1
DVU2560		conserved domain protein	**1.6**	1.3	0.1	-0.7	0.3
DVU2564***	bioF	8-amino-7-oxononanoate synthase	**1.8**	-0.3	0.5	1.1	**2.1**
DVU2571***	feoB	ferrous iron transport protein B	**4.0**	-0.5	-0.3	0.8	**2.2**
DVU2572*	feoA	ferrous iron transport protein A	**4.6**	-0.4	0.2	**2.3**	**3.2**
DVU2573*		hypothetical protein	**3.6**	-0.5	0.2	**1.7**	**3.4**
DVU2574[a]*	feoA	ferrous iron transporter component feoA	**3.0**	-1.3	-0.2	**2.4**	**2.4**
DVU2680[a]*	fld	flavodoxin, iron-repressed	**5.3**	-1.5	-1.0	1.1	**2.4**
DVU2681*		hypothetical protein	**5.0**	-1.3	-1.0	**1.8**	**1.9**
DVU3122		hypothetical protein	**4.4**	0.1	-0.8	0.4	-0.3
DVU3124		hypothetical protein	**1.7**	-1.5	-0.2	1.0	-0.3
DVU3330[a]		hypothetical iron-regulated P-type ATPase	1.4	-0.9	-0.1	0.9	0.3
DVU3331		hypothetical protein	**2.2**	-0.2	0.0	0.9	0.6
DVU3332		heavy metal translocating P-type ATPase	**1.9**	-0.8	-0.5	0.3	-0.2
DVU3333		hypothetical protein	**2.3**	-0.1	-0.2	0.4	0.7
DVU0273[a]***		conserved hypothetical protein	**4.4**	-1.4	-0.6	0.9	1.4
DVU0303*	genZ	hypothetical protein	**4.6**	-0.8	-0.5	**1.8**	**3.2**
DVU0304[a]*	genY	hypothetical protein	**4.5**	-1.0	-0.2	1.5	**3.3**
DVU0251		membrane protein, putative	**2.1**	**2.5**	0.0	-1.1	0.8
DVU2247[b]***	ahpC	alkyl hydroperoxide reductase C	**3.1**	**3.6**	0.4	-0.8	**3.5**
DVU2318[b]***	rbr2	rubrerythrin, putative	**2.1**	**4.6**	0.9	-0.5	**2.9**
DVU0772[b]**		hypothetical protein	0.9	**2.1**	**1.8**	1.5	**5.1**
DVU0712		amino acid ABC transporter, periplasmic-binding protein	0.5	**1.9**	-1.1	**-1.6**	0.1
DVU0881	fusA	translation elongation factor G, putative	1.4	**1.9**	-0.9	-0.8	0.9
DVU1131		hypothetical protein	0.9	**1.8**	0.4	0.0	0.8
DVU1139		bacteriophage DNA transposition B protein, putative	0.5	**1.7**	0.1	0.0	0.2
DVU1141		hypothetical protein	0.9	**2.0**	-0.2	-0.3	0.1
DVU1142		transcriptional regulator, putative	0.1	**1.9**	0.2	0.2	0.2
DVU0231		hypothetical protein	0.7	**1.7**	-0.7	-0.7	-0.3
DVU2688		bacteriophage transposase A protein	0.6	**1.8**	0.5	0.8	0.4
DVU2699	slt	transglycosylase SLT domain protein	0.6	**1.7**	-0.6	-0.7	-1.1
DVU2793		electron transport complex protein RnfD, putative	0.2	**1.6**	-0.1	-0.8	-0.2
DVU3270	cydB	cytochrome d ubiquinol oxidase, subunit II	1.1	**1.7**	-1.1	**-3.5**	-0.4
DVU3271	cydA	cytochrome d ubiquinol oxidase, subunit I	0.8	**1.9**	-0.9	**-2.3**	-0.4
DVU0024**		conserved hypothetical protein	0.4	**2.7**	1.0	-0.2	**2.3**
DVU0172	phsB	thiosulfate reductase (phsB)	1.0	**1.8**	0.7	0.2	0.7
DVU2347	argD	acetylornithine aminotransferase	-0.3	**2.2**	-0.7	-1.5	-0.5
DVU2348	dut	deoxyuridine 5-triphosphate nucleotidohydrolase	-0.2	**2.3**	-0.5	**-2.8**	-1.1
DVU0186		conserved hypothetical protein	0.6	**2.0**	0.9	0.6	0.9

a: containing predicted Fur-binding sites; b: containing predicted PerR-binding sites.

Log_2R ratios of transcriptional response are shown. Boldface indicates more than 3 folds of gene expression change ($|Log2R| \geq 1.6$).

*: Fur-dependent; **: PerR-dependent; ***: PerR and Fur-dependent.

TABLE 3. Up-regulated H_2O_2 responsive genes independent of PerR or FUR (1 mM 120 min vs 0 mM 120 min)

DVU no.	Gene name	Annotated function	Expression ratio in strains		
			WT	ΔperR	Δfur
Cell motility					
DVU2078	cheB-2	protein-glutamate methylesterase CheB	2.2(3.8)	2.3(3.6)	2.7(2.7)
DVU2893	flgG	flagellar basal-body rod protein, putative	1.9(2.6)	3.2(5.8)	2.5(2.8)
Energy production and conversion					
DVU3136	NA	nitroreductase family protein	3.2(4.2)	4.7(7.1)	2.3(1.8)
DVU0665	NA	nitrogen fixation protein nifU	2.2(4.3)	3.7(7.2)	2.6(2.5)
Amino acid transport and metabolism					
DVU0419	nspC	carboxynorspermidine decarboxylase	3.1(4.6)	4.5(7.9)	3.1(2.2)
DVU0421	NA	agmatinase, putative	1.7(2.2)	2.4(3.8)	2.7(2.1)
Posttranslational modification, protein turnover, chaperons					
DVU1457	trxB	thioredoxin reductase, putative	1.9(3.3)	2.5(4.7)	1.7(1.7)
DVU0576	msrB	peptide methionine sulfoxide reductase MsrB	2.9(4.8)	3.7(6.3)	2.7(2.1)
DVU0811	dnaK	dnaK protein	1.7(3.1)	2.6(5.1)	3.1(2.8)
DVU1337	lon	ATP-dependent protease La	1.7(2.7)	2.3(4.4)	2.6(2.0)
DVU1468	htrA	peptidase/PDZ domain protein	2.2(3.5)	1.6(3.0)	1.6(2.3)
DVU1976	groEL	chaperonin, 60 kDa	2.1(3.3)	2.5(4.4)	2.8(2.6)
DVU1977	groES	chaperonin, 10 kDa	2.5(4.5)	3.4(6.4)	3.2(3.2)
DVU2441	hspC	heat shock protein, Hsp20 family	4.7(7.0)	5.4(7.4)	4.0(3.4)
DVU2442	NA	heat shock protein, Hsp20 family	4.9(7.8)	5.4(9.0)	4.9(3.8)
DVU2494	NA	peptidase, M48 family	2.6(4.8)	3.6(5.4)	2.4(2.2)
DVU2643	htpG	heat shock protein HtpG	2.8(4.2)	2.9(5.0)	3.0(3.0)
Signal transduction mechanisms					
DVU2079	NA	sensory box histidine kinase	2.5(4.8)	3.3(6.4)	3.2(3.2)
General function prediction only					
DVU0819	isf-1	FMN reductase, NADPH-dependent	3.1(4.7)	2.9(5.1)	2.4(1.7)
DVU2470	b0786	membrane protein, putaive	1.7(3.0)	2.0(3.6)	2.2(2.2)
DVU2978	NA	hydrolase, haloacid dehalogenase-like family	2.5(4.4)	3.7(6.7)	2.7(2.2)
DVU1430	NA	peptidase, M16 family	2.3(3.5)	2.6(3.3)	2.2(2.0)
DVU1212	fsxA	fxsA protein	1.9(3.6)	3.4(3.9)	2.6(2.1)
DVU3135	mdaB	flavodoxin-like fold domain protein	3.4(4.6)	4.3(7.5)	2.7(1.7)
Function unknown					
DVU1875	NA	dafA protein	2.2(3.9)	2.9(5.2)	1.9(2.4)
DVU0241	NA	MTH1175-like domain family protein	2.2(4.0)	2.4(4.6)	2.7(2.5)
DVU0242	NA	SEC-C motif domain protein	1.6(2.4)	2.0(3.9)	2.3(2.7)
DVU2974	NA	hypothetical protein	2.0(2.6)	2.0(3.1)	1.9(1.6)
DVU2975	NA	hydrolase, putative	2.5(4.6)	3.3(6.0)	2.5(2.5)
DVU2977	NA	hypothetical protein	2.2(3.3)	2.6(4.7)	2.7(2.4)
DVU3346	NA	hypothetical protein	2.3(3.1)	3.2(3.1)	2.0(1.9)
DVU0420	NA	hypothetical protein	2.2(4.2)	3.6(5.2)	2.6(2.1)
DVU0572	NA	hypothetical protein	1.8(2.7)	3.0(5.6)	1.6(1.8)

Log_2R (treatment/control) are shown. Values in parentheses are Z scores.

Supplemental Data

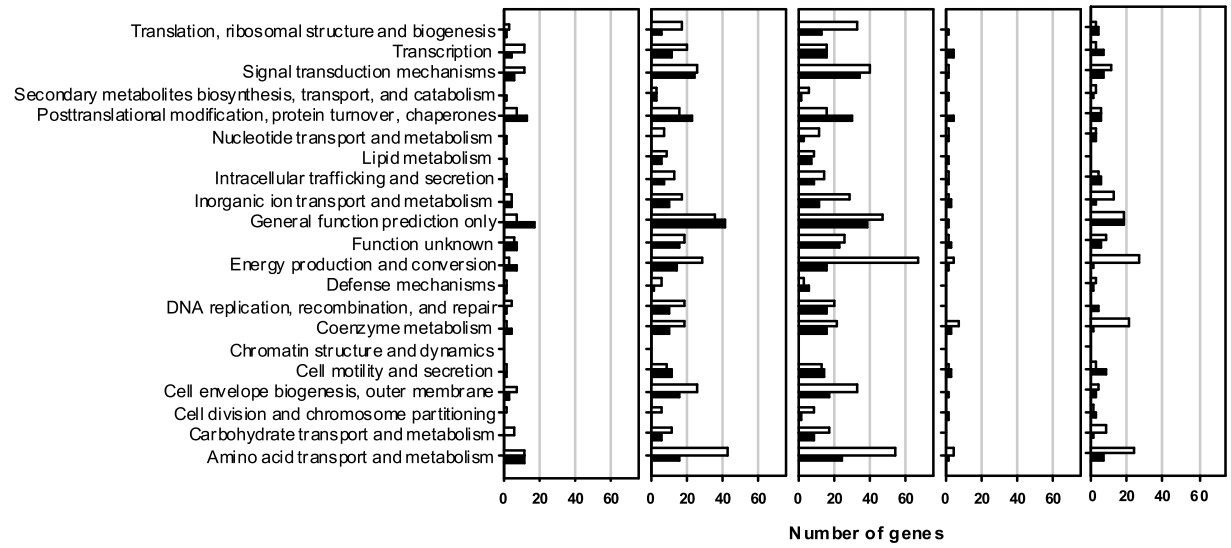

FIG. S1. Profile of the number of genes differentially expressed in the various functional categories by *D. vulgaris* Hildenborough in response to 1 mM H_2O_2 at different time-points after treatment (■: increase of gene expression; □: decrease of gene expression). COG functional categories are those listed.

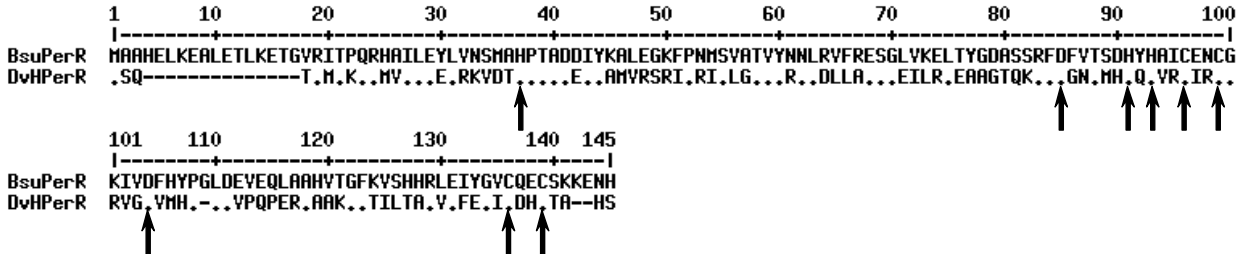

FIG. S2. Alignment of *D. vulagris* PerR and *B. subtilis* PerR. The red color means conserved residues in the protein sequence. The triangles show the conserved amino acids which form the high-affinity Zn^{2+}-binding site (C96, C99, C136 and C139) and candidate ligands for the regulatory ion, Fe^{2+} or Mn^{2+}(H37, D85, H91, H93 and D104).

TABLE S1. Top twenty up-regulated genes at 120 min after 1 mM H_2O_2 treatment

DVU no.	Name	Annotated function	30 min	60 min	120 min	240 min	480 min
DVU0526	NA	drug resistance transporter, putative	0.9 (0.7)	**2.5 (2.2)**	**5.0 (3.5)**	1.0 (0.6)	-0.3 (-0.4)
DVU3136	NA	nitroreductase family protein	**2.2 (4.1)**	**3.8 (6.9)**	**5.0 (9.2)**	**1.3 (1.6)**	0.6 (1.1)
DVU1151	NA	hypothetical protein	**3.2 (2.1)**	**2.5 (2.2)**	**4.6 (3.5)**	1.2 (1.0)	**1.0 (1.6)**
DVU0298	NA	hypothetical protein	**2.9 (4.8)**	**2.8 (5.2)**	**4.4 (7.9)**	**3.2 (2.2)**	0.0 (0.0)
DVU0419	nspC	carboxynorspermidine decarboxylase	**3.1 (6.1)**	**3.6 (7.1)**	**4.3 (8.5)**	**2.3 (2.3)**	0.9 (1.7)
DVU2096	NA	hypothetical protein	-0.1 (-0.2)	**1.4 (2.0)**	**4.1 (2.8)**	0.1 (0.1)	-1.5 (-0.9)
DVU0572	NA	hypothetical protein	**1.8 (3.5)**	**2.7 (5.3)**	**4.1 (7.5)**	**1.3 (1.9)**	0.7 (1.5)
DVU2977	NA	hypothetical protein	**2.6 (4.7)**	**3.6 (6.6)**	**3.9 (7.3)**	**2.5 (1.9)**	0.4 (0.8)
DVU2282	NA	hypothetical protein	**2.3 (4.5)**	**3.2 (5.6)**	**3.9 (7.6)**	**2.2 (1.7)**	0.2 (0.4)
DVU0590	NA	hypothetical protein	**3.1 (5.6)**	**3.6 (4.3)**	**3.6 (6.2)**	**3.0 (1.8)**	-0.1 (-0.1)
DVU2893	flgG	flagellar basal-body rod protein, putative	**2.1 (3.9)**	**2.5 (4.8)**	**3.5 (6.2)**	**1.6 (1.8)**	**1.4 (2.6)**
DVU0728	NA	hypothetical protein	0.1 (0.1)	0.5 (0.4)	**3.5 (5.3)**	1.1 (0.5)	-0.7 (-0.4)
DVU1496	NA	hypothetical protein	0.8 (1.1)	**2.7 (2.1)**	**3.5 (3.0)**	0.3 (0.2)	1.5 (1.4)
DVU3346	NA	hypothetical protein	**2.3 (2.4)**	**2.7 (4.7)**	**3.5 (5.8)**	**2.8 (1.8)**	0.5 (0.8)
DVU2639	NA	conserved hypothetical protein	**1.5 (2.6)**	**1.6 (3.1)**	**3.5 (6.6)**	**2.2 (2.3)**	**1.0 (1.9)**
DVU0727	NA	conserved hypothetical protein	0.6 (1.1)	**1.6 (2.8)**	**3.5 (5.0)**	1.1 (1.3)	0.0 (0.1)
DVU1644	NA	permease, putative	0.9 (1.7)	**1.3 (2.3)**	**3.5 (4.7)**	0.9 (0.9)	-0.0 (-0.0)
DVU2321	NA	hypothetical protein	0.0 (0.0)	**1.0 (1.8)**	**3.4 (5.4)**	1.4 (1.1)	-0.3 (-0.2)
DVU2442	NA	heat shock protein, Hsp20 family	**2.9 (3.4)**	**3.0 (4.3)**	**3.4 (5.4)**	**1.3 (1.9)**	0.9 (1.8)
DVU0359	NA	HesB-like domain	**1.6 (2.5)**	**1.4 (2.1)**	**3.4 (6.2)**	0.6 (0.6)	-1.0 (-1.3)

Top twenty down-reegulated genes at 120 min after 1 mM H_2O_2 treatment

DVU no.	Name	Annotated function	30 min	60 min	120 min	240 min	480 min
DVU0123	NA	membrane protein, putative	-1.2 (-1.1)	-0.6 (-0.5)	**-5.2 (-4.4)**	**-5.6 (-3.3)**	**-6.0 (-3.3)**
DVU1548	NA	outer membrane transport protein, OmpP1/FadL/TodX	-0.1 (-0.2)	**-3.3 (-6.1)**	**-4.3 (-8.0)**	-0.3 (-0.2)	0.5 (0.8)
DVU2803	NA	membrane protein, putative	NA	**-1.4 (-2.4)**	**-3.8 (-4.4)**	-0.8 (-0.6)	-1.3 (-1.8)
DVU3023	atoC	sigma-54 dependent DNA-binding response regulator	**-1.0 (-1.8)**	**-4.3 (-6.1)**	**-3.8 (-6.7)**	-0.5 (-0.3)	-0.9 (-1.2)
DVU0280	wbaZ-2	glycosyl transferase, group 1 family protein	**-1.3 (-2.4)**	**-2.5 (-4.2)**	**-3.7 (-6.1)**	-0.8 (-1.2)	-0.2 (-0.4)
DVU3161	NA	ABC transporter, ATP-binding protein	**-1.6 (-2.7)**	-2.8 (-0.1)	**-3.6 (-6.1)**	-1.1 (-0.8)	-0.1 (-0.1)
DVU1260	NA	outer membrane protein P1, putative	-0.4 (-0.8)	**-2.6 (-4.6)**	**-3.4 (-3.4)**	-0.2 (-0.2)	0.2 (0.3)
DVU2957	NA	hypothetical protein	**-2.8 (-4.7)**	**-4.7 (-8.4)**	**-3.3 (-4.0)**	1.0 (1.2)	-0.3 (-0.5)
DVU2633	NA	transcriptional regulator, putative	**-2.9 (-2.7)**	**-4.1 (-5.2)**	**-3.2 (-4.2)**	0.5 (0.6)	-0.1 (-0.1)
DVU0252	NA	hypothetical protein	-1.5 (-0.0)	**-3.8 (-3.7)**	**-3.1 (-3.7)**	-0.2 (-0.4)	-0.2 (-0.0)
DVU2942	purB	adenylosuccinate lyase	-0.5 (-0.9)	NA	**-3.0 (-3.6)**	NA	-0.2 (-0.4)
DVU1935	phnE	phosphonate ABC transporter, permease protein	**-1.5 (-2.5)**	**-4.5 (-7.2)**	**-3.0 (-4.1)**	-0.3 (-0.1)	0.1 (0.2)
DVU1626	NA	hypothetical protein	**-1.2 (-2.4)**	**-1.8 (-3.2)**	**-3.0 (-4.3)**	-0.8 (-0.7)	0.1 (0.2)
DVU3375	ftsE	cell division ATP-binding protein FtsE, putative	**-1.2 (-2.3)**	-2.6 (-0.1)	**-2.9 (-2.9)**	-0.3 (-0.3)	-0.2 (-0.0)
DVU1650	NA	conserved hypothetical protein	-0.8 (-1.1)	**-1.6 (-2.8)**	**-2.9 (-4.6)**	-0.7 (-0.4)	-0.2 (-0.4)
DVU1464	NA	heptosyltransferase family protein	**-1.2 (-2.2)**	**-2.7 (-4.6)**	**-2.9 (-4.5)**	0.0 (0.1)	-1.0 (-0.0)
DVU2558	bioB	biotin synthase	**-1.0 (-1.5)**	-0.7 (-1.0)	**-2.9 (-4.8)**	-0.6 (-0.0)	**-1.7 (-2.7)**
DVU0670	NA	exopolysaccharide production protein, putative	-0.3 (-0.5)	**-2.2 (-2.8)**	**-2.8 (-4.8)**	0.2 (0.1)	-0.6 (-0.7)
DVU0165	oppF	oligopeptide/dipeptide ABC transporter, ATP-binding	-0.7 (-1.3)	**-1.9 (-3.4)**	**-2.8 (-3.5)**	-0.1 (-0.1)	0.2 (0.4)
DVU3261	frdC	fumarate reductase, cytochrome b subunit	-0.3 (-0.5)	**-2.6 (-3.4)**	**-2.8 (-3.4)**	0.0 (0.0)	-0.6 (-1.0)

Log_2R (treatment/control) ratios of transcriptional response are shown. Values in parentheses are Z scores.

Bold indicates more than two folds of gene expression changes ($|Log_2R| \geq 1$, $|Z| \geq 1.5$).

TABLE S2. The temporal gene expression pattern of selected genes in gene co-expression network

DVU no.	Name	No. of connections	Annotated function	30 min	60 min	120 min	240 min	480 min
Selected genes in Module 1								
DVU0106	glnP	13	glutamine ABC transporter, permease protein (glnP)	**-1.6(-3.1)**	**-2.4(-4.4)**	**-2.2(-3.8)**	-0.3(-0.5)	-0.1(-0.2)
DVU0280	wbaZ-2	13	glycosyl transferase, group 1 family protein	**-1.3(-2.4)**	**-2.5(-4.2)**	**-3.7(-6.1)**	-0.8(-1.2)	-0.2(-0.4)
DVU1655	aspC	8	aminotransferase, classes I and II	**-1.2(-2.4)**	**-1.4(-2.7)**	**-1.8(-2.9)**	0.1(0.2)	-0.2(-0.4)
DVU1144		10	transcriptional regulator, Cro/CI family	**-1.0(-1.7)**	**-2.0(-3.7)**	**-2.1(-3.4)**	0.2(0.4)	0.6(1.2)
DVU0299		12	anaerobic ribonucleoside-triphosphate reductase, putative	-0.8(-1.5)	**-1.6(-2.8)**	**-2.3(-4.2)**	**-1.1(-1.8)**	-0.3(-0.6)
DVU0551	livF	12	high-affinity branched-chain amino acid ABC transporter ATP-binding protein	NA	**-1.8(-3.1)**	**-2.5(-4.0)**	0.5(0.8)	0.1(0.2)
DVU0776	atpG	11	ATP synthase, F1 gamma subunit	-0.6(-1.1)	**-1.1(-2.0)**	**-2.3(-3.7)**	-0.5(-0.5)	-0.1(-0.1)
DVU0777	atpA	11	ATP synthase, F1 alpha subunit	-0.4(-0.7)	**-1.6(-2.9)**	**-2.3(-3.8)**	-0.4(-0.4)	-0.3(-0.5)
DVU1286	dsrP	9	Integral membrane protein	-0.6(-1.2)	**-1.7(-3.2)**	**-2.3(-4.1)**	-0.6(-0.7)	0.1(0.2)
DVU1287	dsrO	3	Periplasmic (Tat), binds 2[4Fe-4S]	-0.4(-0.8)	-0.7(-1.4)	**-1.3(-2.2)**	-0.2(-0.2)	0.0(0.0)
DVU1288	dsrJ	9	Periplasmic (Sec) triheme cytochrome c	-0.2(-0.4)	**-1.0(-1.8)**	**-1.7(-2.9)**	-0.4(-0.5)	-0.0(-0.1)
DVU1289	dsrK	4	Cytoplasmic, binds 2 [4Fe-4S]	-0.2(-0.4)	-0.8(-1.5)	**-1.3(-2.0)**	-0.2(-0.2)	-0.0(-0.1)
DVU1290	dsrM	1	Inner membrane protein binds 2 heme b	0.1(0.2)	**-1.2(-2.3)**	**-2.2(-3.6)**	0.1(0.1)	0.1(0.2)
DVU1204	fabF	10	3-oxoacyl-(acyl-carrier-protein) synthase II	-0.5(-0.9)	**-1.1(-1.9)**	**-1.6(-2.6)**	-0.1(-0.2)	0.2(0.5)
DVU2225		7	acetyl-CoA carboxylase, carboxyl transferase, alpha/beta subunit	-0.7(-1.2)	**-1.4(-2.5)**	**-2.7(-3.7)**	-0.6(-0.6)	0.1(0.2)
DVU2226	accC	7	acetyl-CoA carboxylase, biotin carboxylase, putative	-0.5(-1.0)	**-1.2(-2.2)**	**-1.3(-2.4)**	-0.3(-0.4)	-0.4(-0.8)
DVU1309	rpsC	9	ribosomal protein S3	-0.3(-0.6)	**-1.0(-2.0)**	**-1.1(-2.1)**	-0.0(-0.0)	0.0(0.1)
DVU2924	rplK	6	ribosomal protein L11	-0.5(-0.9)	-1.2(-0.0)	**-1.8(-3.4)**	-0.1(-0.2)	0.1(0.2)
DVU1310	rplP	9	ribosomal protein L16 (rplP)	-0.5(-0.9)	**-1.0(-1.9)**	**-1.6(-2.9)**	-0.3(-0.4)	0.0(-0.1)
DVU1311	rpmC	8	ribosomal protein L29 (rpmC)	-0.4(-0.7)	-0.9(-1.6)	**-1.3(-2.2)**	-0.2(-0.3)	0.2(0.3)
DVU0758		11	hypothetical protein	**1.4(2.0)**	**1.4(2.6)**	**2.5(4.2)**	1.4(1.1)	-0.3(-0.5)
DVU0665	NA	12	nitrogen fixation protein nifU	**1.6(2.9)**	**2.1(3.6)**	**2.4(4.6)**	0.7(1.3)	0.5(1.0)
DVU1457	trxB	8	thioredoxin reductase, putative	**1.2(2.1)**	**1.8(3.4)**	**2.2(4.2)**	1.1(1.0)	0.0(0.1)
DVU1601	NA	8	ATP-dependent Clp protease adaptor protein ClpS	**1.4(2.5)**	**1.9(3.6)**	**2.8(5.1)**	1.5(1.4)	0.5(1.0)
DVU1875	NA	7	dafA protein	**2.1(3.1)**	**2.7(4.7)**	**3.3(6.2)**	1.6(1.2)	-0.0(-0.0)
DVU1876	dnaJ	7	dnaJ protein, putative	**1.9(3.6)**	**2.7(5.0)**	**3.0(5.1)**	1.4(1.3)	0.2(0.3)
DVU1984	msrA	7	peptide methionine sulfoxide reductase MsrA	**1.2(2.2)**	**2.0(3.6)**	**3.0(6.0)**	**1.4(1.5)**	0.2(0.3)
DVU0576	msrB	5	peptide methionine sulfoxide reductase MsrB	**3.0(5.0)**	**3.2(5.6)**	**3.0(5.5)**	**2.1(1.7)**	0.3 (0.5)
DVU2282	NA	6	hypothetical protein	**2.3(4.5)**	**3.2(5.6)**	**3.9(7.6)**	**2.2(1.7)**	0.2(0.4)
DVU2310	NA	6	metallo-beta-lactamase family protein	**2.3(3.8)**	**2.7(4.7)**	**3.3(5.7)**	**1.9(1.6)**	0.4(0.8)
DVU0758	NA	11	hypothetical protein	**1.4(2.0)**	**1.4(2.5)**	**2.5(4.1)**	1.4(1.0)	-0.3(-0.5)
DVU1193	radC	5	DNA repair protein RadC	**1.0(1.8)**	**1.4(2.6)**	**2.4(4.4)**	1.3(1.3)	-0.0(-0.0)
DVU3136	NA	6	nitroreductase family protein	**2.2(4.1)**	**3.8(7.0)**	**5.0(9.2)**	**1.3(1.6)**	0.6(1.1)
Module 2								
DVU2494	NA		peptidase, M48 family	**2.4(3.6)**	**2.0(3.6)**	**2.2(4.2)**	**2.3(1.9)**	0.5(1.0)
DVU1468	htrA		peptidase/PDZ domain protein	**1.4(2.4)**	**1.5(2.9)**	**1.8(3.3)**	**1.2(1.3)**	-0.0(-0.0)
DVU2571	feoB		ferrous iron transport protein B	**1.1(1.8)**	**1.2(2.3)**	**1.7(3.1)**	**1.9(1.5)**	0.5(0.9)
DVU0241	NA		MTH1175-like domain family protein	**1.2(2.1)**	**1.6(3.0)**	**1.9(3.7)**	**1.0(1.7)**	-0.0(-0.0)
DVU0242	NA		SEC-C motif domain protein	0.9(1.7)	**1.1(2.0)**	**1.8(3.5)**	0.7(1.1)	-0.1(-0.2)
Module 3								
DVU3030	ackA		acetate kinase	-0.8(-1.4)	**-0.7(-1.5)**	**-2.2(-4.2)**	-1.1(-1.4)	-0.6(-1.2)
DVU3032	NA		conserved hypothetical protein	-0.1(-0.2)	-0.4(-0.8)	**-2.1 (-3.6)**	-0.8(-1.1)	-0.4(-0.7)
DVU3033	NA		iron-sulfur cluster-binding protein	-0.2(-0.3)	-0.4(-0.8)	**-1.5(-2.7)**	-0.9(-1.2)	-0.3(-0.6)
DVU3093	rdl		rubredoxin-like protein	0.5(0.9)	0.9(1.7)	**1.7(3.0)**	0.8(1.0)	0.3(0.5)
Module 4								
DVU2794	NA		NADH:quinone oxidoreductase subunit RnfG	0.2(0.4)	**-0.2(-0.4)**	**-1.6(-2.7)**	-0.7(-1.1)	-0.9(-1.7)
DVU0264	tmcB		Transmembrane complex, ferredoxin, 2 [4Fe-4S]	0.1(0.1)	-0.2(-0.4)	**-1.0(-1.9)**	-0.5(-0.9)	-0.7(-1.3)
DVU0263	tmcA		Transmembrane complex, tetraheme cytochrome c3	0.0(0.1)	**0.0(0.0)**	**-0.9(-1.6)**	-0.2(-0.4)	-0.6(-1.2)
DVU0260	mtrA		response regulator	-0.1(-0.1)	**-0.5(-0.9)**	**-1.3(-2.4)**	-0.6(-1.1)	-0.7(-1.4)
DVU0035	NA		hypothetical protein	0.2(0.4)	0.6(1.1)	**2.0(3.9)**	0.5(0.7)	0.6(1.1)
Module 5								
DVU2077	NA		conserved hypothetical protein	-0.2(-0.3)	**-1.0(-1.9)**	**-1.8(-3.0)**	-0.6(-0.9)	-0.7 (-1.4)
DVU2078	cheR-2		chemotaxis protein methyltransferase	-0.4(-0.8)	**-1.1(-2.1)**	**-1.5(-2.7)**	-0.6(-0.9)	-0.8(-1.5)
DVU2288	NA		hydrogenase, CooL subunit, putative	-0.3(-0.6)	-0.5(-1.0)	**-1.3(-2.4)**	-0.5(-0.7)	-0.7(-1.5)
DVU2289	b2488		hydrogenase, CooX subunit, putative	-0.4(-0.7)	-0.7(-1.4)	**-1.3(-2.2)**	-0.5(-0.8)	-0.8(-1.5)
DVU0657	NA		heat shock protein, Hsp20 family	-0.1(-0.1)	-0.8(-1.4)	**-1.3(-2.2)**	-0.6(-1.0)	-0.7(-1.4)
DVU2330	NA		MRP family protein	-0.4(-0.8)	-0.9(-1.7)	**-1.7(-3.0)**	-0.3(-0.4)	-0.4(-0.9)
DVU3174	ubiE		ubiquinone/menaquinone biosynthesis methlytransferase UbiE	-0.2(-0.4)	**-1.2(-2.2)**	**-2.1(-3.3)**	-0.0(-0.0)	-0.4(-0.7)
DVU2070	NA		TPR domain protein	-0.3(-0.5)	-0.6(-1.1)	**-1.3(-2.2)**	-0.5(-0.6)	-0.6(-1.2)

Log_2R (treatment/control) ratios of transcriptional response are shown. Values in parentheses are Z scores.
Bold indicates more than two folds of gene expression changes($|Log_2R| \geq 1$, $|Z| \geq 1.5$).